BULLETIN (New Series) OF THE AMERICAN MATHEMATICAL SOCIETY Volume 60, Number 2, April 2023, Pages 195–250 https://doi.org/10.1090/bull/1782 Article electronically published on November 28, 2022

BILLIARDS AND TEICHMÜLLER CURVES

CURTIS T. MCMULLEN

ABSTRACT. A Teichmüller curve $V \subset \mathcal{M}_g$ is an isometrically immersed algebraic curve in the moduli space of Riemann surfaces. These rare, extremal objects are related to billiards in polygons, Hodge theory, algebraic geometry and surface topology. This paper presents the six known families of primitive Teichmüller curves that have been discovered over the past 30 years, and a selection of open problems.

1. Introduction

The moduli space \mathcal{M}_g of compact Riemann surfaces of genus g is both a metric space and an algebraic variety.

The metric comes from the *Teichmüller distance* between $X,Y\in\mathcal{M}_g$, which measures the minimal conformal distortion of a map $f:X\to Y$. This metric is given by a norm on each tangent space to \mathcal{M}_g , but for g>1 it is not Riemannian; in fact the norm balls are complicated convex sets, varying so much from point to point that \mathcal{M}_g is completely inhomogeneous.

The algebraic structure on \mathcal{M}_g comes from a projective embedding, which provides a multitude of algebraic curves $V \subset \mathcal{M}_g$. Each curve carries a natural hyperbolic metric, coming from its uniformization $V = \mathbb{H}/\Gamma$.

We say $V \subset \mathcal{M}_g$ is a *Teichmüller curve* if this inclusion is an *isometry*. These rare and remarkable objects lie at the nexus of algebraic geometry, number theory, complex analysis, topology and automorphic forms. We focus on *primitive* examples, since all others are related to these by covering constructions (§2).

Teichmüller curves are elusive, but once found, they can often be viewed explicitly from many perspectives at once. For example, any primitive Teichmüller curve V determines a totally real number field K, with $\deg(K/\mathbb{Q}) \leq g$, such that:

- $V \cong \mathbb{H}/\Gamma$, with $\Gamma \subset \mathrm{SL}_2(K)$;
- every Riemann surface $X \in V \subset \mathcal{M}_g$ can be assembled from triangles with vertices in $K \oplus K\tau \subset \mathbb{C}$, for some $\tau \in \mathbb{H}$; and
- \bullet a factor of the Jacobian of X admits real multiplication by K.

The curve V is rigid, so both V and its map to \mathcal{M}_g are also defined over a number field. In particular cases one can obtain algebraic equations for V, generators for Γ , and geometric models for X and for endomorphisms of its Jacobian.

Received by the editors November 2, 2021. 2020 Mathematics Subject Classification. Primary 32G15. The author's research was supported in part by the NSF.

©2022 Curtis T. McMullen

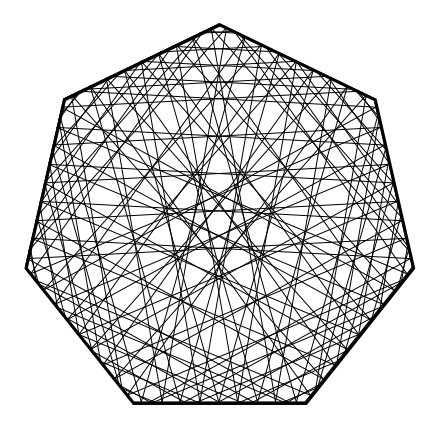


FIGURE 1.1. A periodic billiard trajectory in the regular heptagon.

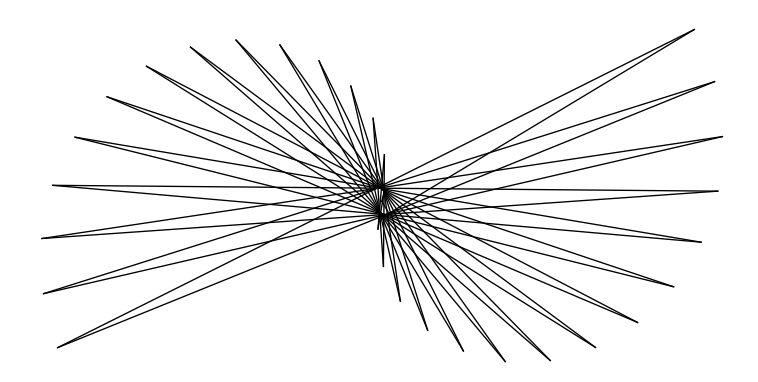


FIGURE 1.2. A generalized billiard table with optimal dynamics.

Billiards. Frequently $X \in V$ can be chosen so there is a polygon P and a finite reflection group G, adapted to V, such that

$$X/G \cong P \subset \mathbb{C}$$
.

In this case, billiards in the polygon P has $optimal\ dynamics$: every trajectory is either periodic, or uniformly distributed. Moreover, X and V can be reconstructed from P.

The regular polygons provide the first examples of both optimal billiards and Teichmüller curves (see Figure 1.1 and $\S 3$). It is also possible that P is immersed, rather than embedded in \mathbb{C} ; in this case we obtain a generalized polygon with optimal dynamics (see Figure 1.2 and $\S 7$).

The current catalog. This paper provides a survey of the known examples of Teichmüller curves, a glimpse of their multifaceted constructions, a hint of how they were discovered, and a selection of the many open questions that remain.

The known primitive Teichmüller curves are given by 6 infinite series, and 3 sporadic examples. These are:

- 1. the three Weierstrass series W_D , in genus 2, 3 and 4 (§4, §5);
- 2. the sporadic examples of type E_6 , E_7 and E_8 , in genus 3 and 4 (§6);

- 3. the Bouw–Möller series $V_{p,q}$, providing finitely many examples in every \mathcal{M}_g (§7); and
- 4. the gothic and arabesque series, G_D and A_D , both in genus 4 (§8, §9).

The five horizontal series W_D , G_D and A_D above each lie in a single moduli space. The index D is a real quadratic discriminant, i.e. an integer D > 0, D = 0 or $1 \mod 4$, with $\sqrt{D} \notin \mathbb{Z}$.

Completeness? In low genus, the list of primitive Teichmüller curves is almost complete.

- In genus g=2, all primitive Teichmüller curves are known: they are accounted for by the series $W_D \subset \mathcal{M}_2$ and one other curve, associated to billiards in the regular decagon (Theorem 4.5).
- In genus g = 3, there are only finitely many primitive Teichmüller curves not accounted for by the series $W_D \subset \mathcal{M}_3$ (Theorem 5.5).

On the other hand, the *vertical* Bouw–Möller series V_{pq} gives the *only known* construction of primitive Teichmüller curves in genus $g \geq 5$. Thus a central open problem is to settle:

Question 1.1. Are there infinitely many primitive Teichmüller curves in \mathcal{M}_5 ?

The unexpected families G_D and A_D in genus 4 hint that similar constructions may be hidden in higher genus.

Teichmüller surfaces. The discovery of the gothic curves G_D also revealed an almost miraculous new phenomenon: there are primitive, totally geodesic *Teichmüller surfaces* in $\mathcal{M}_{1,3}$, $\mathcal{M}_{1,4}$ and $\mathcal{M}_{2,1}$. This survey concludes with a description of these new surfaces from the perspective of algebraic geometry in §8, and from the perspective of quadrilaterals in §9.

Notes and references. References and commentary are collected, section by section, in §10.

Via the action of $SL_2(\mathbb{R})$ on $\Omega \mathcal{M}_g$, Teichmüller curves are connected to the larger topic of dynamics on moduli spaces, which is itself patterned on the theory of homogeneous dynamics, Lie groups, lattices and ergodic theory. For a view of the broader setting, we recommend the many excellent surveys such as [D], [Go], [HS2], [Mas3], [MT], [Mo3], [Sch2], [Vo1], [Wr2], [Wr3], [Y], and [Z].

Outline. In §2 and §3 we set the stage with definitions and basic examples regarding moduli spaces, polygons and billiards. The known families of primitive Teichmüller curves are described in §4 through §9.

Four appendices follow. The triangle groups $\Delta(p, q, \infty) \subset SL_2(\mathbb{R})$ are reviewed in Appendix A. There are six accidental isomorphisms between members of series of Teichmüller curves listed above; these are recorded in Appendix B. Tables of invariants of Teichmüller curves appear in Appendices C and D.

Notation. The *n*th Chebyshev polynomial will be denoted by $T_n(x) \in \mathbb{Z}[x]$; it is characterized by

$$(1.1) T_n(\cos \theta) = \cos(n\theta).$$

We let $H^1(X)$ denote cohomology with complex coefficients. The upper half-plane in $\mathbb{H} = \{z : \operatorname{Im}(z) > 0\} \subset \mathbb{C}$ is endowed with the complete hyperbolic metric

$$\rho_{\mathbb{H}} = \frac{|dz|}{2 \operatorname{Im} z}$$

of constant curvature -4. The group $SL_2(\mathbb{R})$ acts linearly on $\mathbb{R}^2 \cong \mathbb{C}$ and by Möbius transformations on \mathbb{H} .

2. Moduli spaces and Teichmüller curves

This section develops background material on Riemann surfaces, polygons, and the action of $SL_2(\mathbb{R})$ on the moduli space of holomorphic 1-forms $\Omega \mathcal{M}_g$. This material will allow us to formulate the main topic we aim to address:

Problem 2.1. Construct and classify all primitive Teichmüller curves $V \to \mathcal{M}_q$.

Moduli space. The moduli space \mathcal{M}_g parameterizes the isomorphism classes of compact Riemann surfaces X of genus g. It is naturally a complex orbifold, and an algebraic variety, of complex dimension 3g-3 when $g \geq 2$.

The *Teichmüller metric* on \mathcal{M}_g is defined by a norm on each tangent space; it can be characterized as the largest metric such that every holomorphic map

$$(2.1) f: \mathbb{H} \to \mathcal{M}_q$$

is either a contraction or an isometry. In the isometric case, we say f is a complex geodesic.

Metrically, moduli space is completely inhomogeneous: the tangent spaces at $X, Y \in \mathcal{M}_g$ are isomorphic as normed vector spaces if and only if X = Y. Nevertheless, there exists a unique complex geodesic through every point in every possible direction

Polygons and Riemann surfaces. How can one specify a Riemann surface $X \in \mathcal{M}_g$?

In the case g=1, X is a torus, thus one can write $X=\mathbb{C}/\Lambda$ for some lattice $\Lambda\subset\mathbb{C}$. Alternatively, if we choose a parallelogram $P\subset\mathbb{C}$ that is a fundamental domain for the action of Λ , we can construct X by gluing together opposite sides of P.

More generally, if $P \subset \mathbb{C}$ is any polygon, and the edges of P are identified in pairs by *translations*, then the result is a compact Riemann surface $X = P/\sim$. And in fact:

Every compact Riemann surface of genus $g \ge 1$ can be presented as a polygon $P \subset \mathbb{C}$ with its edges glued together by translations.

Note that X inherits a flat metric from P. At first sight this may seem paradoxical: for $g \geq 2$, X admits no smooth flat metric. However the metric on X has, in general, isolated singularities of negative curvature arising from the vertices of P.

Example in genus 2. Consider the polygon L(a,b) shown in Figure 2.1. Note that we have introduced two extra vertices, so L(a,b) is combinatorially an octagon. Gluing edges by vertical and horizontal translations, we obtain a Riemann surface X of genus 2. The eight vertices of L(a,b) descend to a single point $p \in X$; there, the induced flat metric has a cone angle of 6π .

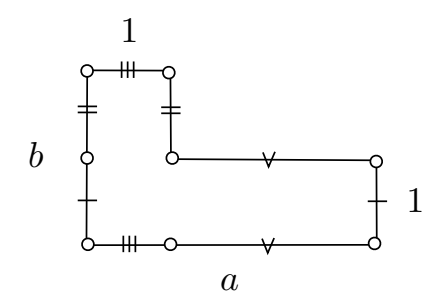


FIGURE 2.1. The polygon L(a,b) glues up to give a Riemann surface of genus 2.

Holomorphic 1-forms. This *flat uniformization* of X by a polygon P can be contrasted with more traditional ways of presenting a compact Riemann surface, e.g. as an algebraic curve or as a quotient of $\mathbb H$ by a Fuchsian group. While a polygonal presentation of X is elementary, it is not canonical; moreover, it provides X with additional structure.

To explain this, recall that the space $\Omega(X)$ of holomorphic 1-forms ω on X has dimension g; indeed, dim $\Omega(X)$ can be taken as the definition of the genus g of X. In local coordinates, $\omega = \omega(z) \, dz$, where $\omega(z)$ is a holomorphic function. Provided $\omega \neq 0$, its zero set $Z(\omega) \subset X$ consists of 2g-2 points, counted with multiplicity.

The moduli space of all nonzero 1-forms (X, ω) of genus g forms a bundle

$$\Omega \mathcal{M}_q \to \mathcal{M}_q$$
;

in fact, it is a holomorphic vector bundle of rank q with its zero section removed.

Strata. The locus where the zeros of ω have multiplicities $p=(p_1,\ldots,p_n)$ forms a stratum

$$\Omega \mathcal{M}_q(p_1,\ldots,p_n) \subset \Omega \mathcal{M}_q$$

of dimension 2g+n-1. These strata decompose $\Omega \mathcal{M}_g$ into disjoint algebraic sets, indexed by the partitions p of 2g-2. We sometimes use exponential notation for repeated blocks of a partition; e.g. the unique open stratum is denoted by $\Omega \mathcal{M}_g(1^{2g-2}) = \Omega \mathcal{M}_g(1,1,\ldots,1)$.

From polygons to 1-forms. Let $X = P/\sim$. Since the 1-form dz on \mathbb{C} is invariant under translation, it descends to give a 1-form $\omega \in \Omega(X)$. Here is a more precise description of the relationship between Riemann surfaces and polygons.

Theorem 2.2. Every element of $\Omega \mathcal{M}_q$ can be presented in the form

$$(2.2) (X,\omega) = (P,dz)/\sim$$

for a suitable polygon $P \subset \mathbb{C}$.

It is often useful, as we will see below, to allow the 'polygon' P to be disconnected. With this proviso, the proof of the result above is fairly elementary: one can construct a geodesic triangulation of the flat surface $(X, |\omega|)$, with $Z(\omega)$ among its vertices, and then present X as the quotient of a collection of Euclidean triangles.

Geometry of a 1-form. A holomorphic 1-form provides X with a singular flat metric $|\omega|$. This metric has a cone angle of $2\pi(p+1)$ at each zero of order p. The form $|\omega|^2$ determines a smooth measure on X, with total mass given by

$$\operatorname{area}(X,\omega) = \int_X |\omega|^2 = \operatorname{area}(P).$$

Near any point $p \notin Z(\omega)$, we can choose a local flat coordinate $z(q) = \int_p^q \omega$ on X such that $\omega = dz$. The geodesics on $(X, |\omega|)$ are simply straight lines in these charts. Since these flat coordinates are well-defined up to translation, each geodesic γ has a well-defined slope s. In particular, γ cannot cross itself; all geodesics are simple. We allow a geodesic to begin or end at a point of $Z(\omega)$, but never to pass through a zero. In particular, a closed geodesic is always disjoint from $Z(\omega)$.

These features are elementary to see in a polygonal model $(X, \omega) = (P, dz)/\sim$; for example, the horizontal lines in P descend to a foliation $\mathcal{F}(\omega)$ of X by geodesics with slope zero. Intrinsically, this foliation is defined by the closed 1-form $\beta = \operatorname{Im} \omega$.

A cylinder $C \subset X$ is the closure of a maximal open set foliated by parallel closed geodesics. Every closed geodesic γ lies in a cylinder; in particular, γ is never unique its homotopy class. Most elements of $\pi_1(X)$ are not represented by closed geodesics; rather, the loop of minimal length in a given homotopy class is a chain of geodesic segments of varying slopes, with endpoints in $Z(\omega)$.

Action of $SL_2(\mathbb{R})$. Remarkably, upon passage to the bundle $\Omega \mathcal{M}_g$, the highly inhomogeneous space \mathcal{M}_g acquires a *dynamical character*: namely, it admits a natural action of $SL_2(\mathbb{R})$. This action is easily described in terms of a polygonal presentation (2.2): for $A \in SL_2(\mathbb{R})$, we have:

$$A \cdot (X, \omega) = (X_A, \omega_A) = (A(P), dz) / \sim.$$

Here A acts linearly on $P \subset \mathbb{C} \cong \mathbb{R}^2$, and the (combinatorial) gluing instructions remains the same.

Alternatively, given $A = \begin{pmatrix} a & b \\ c & d \end{pmatrix}$ one can define a harmonic form on X by

$$\omega_A = \begin{pmatrix} 1 & i \end{pmatrix} \begin{pmatrix} a & b \\ c & d \end{pmatrix} \begin{pmatrix} \operatorname{Re} \omega \\ \operatorname{Im} \omega \end{pmatrix},$$

and then change the complex structure on X so ω_A is holomorphic on X_A . The zeros of ω and ω_A have the same order, so:

 $SL_2(\mathbb{R})$ leaves each stratum $\Omega \mathcal{M}_q(p)$ invariant.

Complex geodesics. Note that if $A \in SO_2(\mathbb{R})$ is simply a rotation, then $X_A = X$ and $\omega_A = \exp(i\theta)\omega$ for some θ . Thus the projection of $A \cdot (X, \omega)$ to \mathcal{M}_g depends only on the coset

$$[A] \in SO_2(\mathbb{R}) \setminus SL_2(\mathbb{R}) \cong \mathbb{H},$$

and the map $F(A) = (X_A, \omega_A)$ covers a unique map $f : \mathbb{H} \to \mathcal{M}_g$, making the diagram

(2.4)
$$\operatorname{SL}_{2}(\mathbb{R}) \xrightarrow{F} \Omega \mathcal{M}_{g}$$

$$\downarrow \qquad \qquad \downarrow^{\pi}$$

$$\mathbb{H} \xrightarrow{f} \mathcal{M}_{g}$$

commute.



FIGURE 2.2. The $SL_2(\mathbb{R})$ -orbit of L(a,b) defines a complex geodesic in \mathcal{M}_2 .

The map f is a holomorphic, isometric immersion of $\mathbb H$ into moduli space, which we refer to as the *complex geodesic* generated by (X,ω) . If $X=P/\sim$, then the image of f simply consists of all Riemann surfaces of the form $X_A=A(P)/\sim$, $A\in \mathrm{SL}_2(\mathbb R)$; see Figure 2.2.

Real geodesics. Every 1-form also generates a distinguished *real* Teichmüller geodesic ray $\gamma:[0,\infty)\to\mathcal{M}_q$; parameterized by arclength, it is given by

$$\gamma(t) = f(ie^{2t}) = X_t,$$

where

$$(X_t, \omega_t) = \begin{pmatrix} e^{-t} & 0 \\ 0 & e^t \end{pmatrix} \cdot (X, \omega).$$

The Riemann surface X_t is obtained from $(X, |\omega|)$ by shrinking its horizontal geodesics and expanding its vertical ones.

Teichmüller curves. The stabilizer of (X, ω) is a discrete subgroup

$$\mathrm{SL}(X,\omega)\subset\mathrm{SL}_2(\mathbb{R}).$$

It is easy to see that the complex geodesic generated by (X, ω) descends to give a map $f: V \to \mathcal{M}_q$, where

$$(2.6) V = \mathbb{H}/\operatorname{SL}(X, \omega).$$

Here the action of $SL(X, \omega)$ on \mathbb{H} is slightly twisted, since $SO_2(\mathbb{R})$ acts on the left in equation (2.3); it is given by A(z) = (az - b)/(-cz + d).

Now suppose V has finite hyperbolic area; equivalently, suppose $SL(X, \omega)$ is a lattice in $SL_2(\mathbb{R})$. Then the image of the map

$$f:V\to\mathcal{M}_q$$

is a *Teichmüller curve* in \mathcal{M}_g . That is, V is the normalization of a totally geodesic algebraic curve.

We refer to (X, ω) as a generator of the Teichmüller curve V. The generator of V is not unique—for any $\lambda \in \mathbb{C}^*$ and $A \in \mathrm{SL}_2(\mathbb{R})$, V is also generated by $A \cdot (X, \lambda \omega)$.

Hidden symmetries. The pivotal group $SL(X, \omega)$ —which is large in the case of a Teichmüller curve—reflects hidden symmetries of the form (X, ω) itself.

More precisely, $\mathrm{SL}(X,\omega)$ can be described as follows. Let $\mathrm{Aff}^+(X,\omega)$ denote the group of orientation–preserving homeomorphisms of X that stabilize $Z(\omega)$, and have the form

$$\phi(x,y) = A \begin{pmatrix} x \\ y \end{pmatrix} + b$$

in local flat coordinates z=x+iy on the domain and range satisfying $\omega=dz$. Here $A\in \mathrm{SL}_2(\mathbb{R})$ and $b\in \mathbb{R}^2$.

We refer to ϕ as an affine automorphism of (X, ω) , since it preserves the realaffine structure on X determined by ω ; in particular, ϕ sends geodesics to geodesics.

The matrix $A = D\phi$ is independent of the choice of charts, and is characterized by
the property that

(2.7)
$$\phi^*(\omega) = \begin{pmatrix} 1 & i \end{pmatrix} A \begin{pmatrix} \operatorname{Re} \omega \\ \operatorname{Im} \omega \end{pmatrix}.$$

In particular, A = I if and only if ϕ belongs to $\operatorname{Aut}(X, \omega)$, the group of holomorphic automorphisms of X satisfying $\phi^*(\omega) = \omega$.

It is then easy to see we have an exact sequence:

$$1 \to \operatorname{Aut}(X, \omega) \to \operatorname{Aff}^+(X, \omega) \xrightarrow{D} \operatorname{SL}(X, \omega) \to 1.$$

For g > 1, the group $\operatorname{Aut}(X, \omega)$ is finite, so the stabilizer of (X, ω) in $\operatorname{SL}_2(\mathbb{R})$ is virtually the same as its affine symmetry group.

Examples. The square torus $E = \mathbb{C}/\mathbb{Z}[i]$ generates the simplest example of a Teichmüller curve. In this case, every orientation–preserving automorphism of $E \cong \mathbb{R}^2/\mathbb{Z}^2$ as a Lie group is also an affine automorphism of (E, dz). Thus $\mathrm{SL}_2(E, dz) = \mathrm{SL}_2(\mathbb{Z})$, and the map $f: V \to \mathcal{M}_1$ is an isomorphism. This is the *trivial Teichmüller curve*.

An example in genus two is provided by the form $(Y, \eta) = L(2, 2)/\sim$ (see Figure 2.1). Here we find

(2.8)
$$\operatorname{SL}(Y,\eta) = \langle S, T \rangle = \left\langle \begin{pmatrix} 0 & 1 \\ -1 & 0 \end{pmatrix}, \begin{pmatrix} 1 & 2 \\ 0 & 1 \end{pmatrix} \right\rangle \subset \operatorname{SL}_2(\mathbb{Z}).$$

In these examples $\mathrm{SL}(E,dz)$ and $\mathrm{SL}(Y,\eta)$ are both triangle groups, namely $\Delta(2,3,\infty)$ and $\Delta(2,\infty,\infty)$. See Appendix A for more on triangle groups, which will occur frequently in the discussions to follow.

Cylinders and parabolics. The modulus of a cylinder of height h and circumference c is m = h/c. In general, if $(X, |\omega|)$ is covered by a collection of n horizontal cylinders (C_i) with moduli (m_i) , and m > 0 divides m_i for all i (meaning m_i/m is an integer), we can construct an affine automorphism ϕ of (X, ω) with

$$D\phi = \begin{pmatrix} 1 & 1/m \\ 0 & 1 \end{pmatrix}.$$

Namely we take $\phi|C_i$ to be a linear, right Dehn twist, iterated m_i/m times. The iterate is chosen so $D\phi|C_i$ is the matrix above for all i. Since $\phi|C_i$ is the identity on ∂C_i , these twists fit together to give a map $\phi \in \text{Aff}^+(X,\omega)$.

Conversely, it is not hard to show:

Proposition 2.3. Suppose $SL(X,\omega)$ contains a parabolic element A fixing the line of slope s through the origin. Then (X,ω) is tiled by a family of cylinders (C_1,\ldots,C_n) of slope s, with rational ratios of moduli.

We can now explain the appearance of the parabolic matrix $T = \begin{pmatrix} 1 & 2 \\ 0 & 1 \end{pmatrix}$ in $SL(Y, \eta)$. Note that L(2, 2) is built from three copies of the unit square. The bottom two squares define a horizontal cylinder $C_1 \subset Y$, isometric to a Euclidean

cylinder of height and circumference $(h_1, c_1) = (1, 2)$. Similarly the top square gives a cylinder C_2 with $(h_2, c_2) = (1, 1)$. Thus $m = \gcd(m_1, m_2) = \gcd(1/2, 1) = 1/2$, and $D\phi = \begin{pmatrix} 1 & 2 \\ 0 & 1 \end{pmatrix}$.

As for the generator S, it is easy to see that $L(a,b)/\sim$ has a 4-fold rotational symmetry whenever a=b (see Figure 3.4).

Cusps of V. We note that the Teichmüller curve V generated by a 1-form (X, ω) is properly immersed in \mathcal{M}_g , and hence the $\mathrm{SL}_2(\mathbb{R})$ orbit of (X, ω) in $\Omega \mathcal{M}_g$ is closed.

Proposition 2.4. A Teichmüller curve V has finite hyperbolic area, but it is never compact; it always has at least one cusp.

Idea of the proof. Assume $g \geq 2$ and $(X, \omega) \in \Omega \mathcal{M}_g(p)$. Construct a geodesic segment σ on $(X, |\omega|)$ with endpoints in $Z(\omega)$. After rotating ω , we can assume σ is horizontal. Now consider the Teichmüller geodesic ray $X_t = \gamma(t)$ in V generated by (X, ω) , as in equation (2.5). As $t \to \infty$ the length of δ on X_t tends to zero. Since the $\mathrm{SL}_2(\mathbb{R})$ orbit of (X, ω) is closed in its stratum, the endpoints of δ cannot collide, so X_t tends to infinity in \mathcal{M}_g . Therefore V is noncompact, and X_t tends to a cusp of V.

Combined with Proposition 2.3, we find that (X, ω) has many cylinder decompositions and a dense set of periodic directions.

Square—tiled surfaces. Let us say (X, ω) is a square–tiled 1-form if it can be obtained by gluing together a finite number of copies of the unit square $([0, 1]^2, dz)$.

Generalizing the case of $(Y, \eta) = L(2, 2)/\sim$, one can show that $SL(X, \omega)$ has finite index in $SL_2(\mathbb{Z})$ for any square–tiled 1-form. One can also check that square tiled surfaces are dense in \mathcal{M}_q . Consequently:

Teichmüller curves are dense in \mathcal{M}_q .

These Teichmüller curves, however, are simply *echos* in higher genus of the trivial Teichmüller curve $V \cong \mathcal{M}_1$. Every Teichmüller curve generates similar echos in higher genus, via covering constructions. For example, there is a degree 3 holomorphic map $f: Y \to E$ such that $\eta = f^*(dz)$.

Primitivity. For this reason we will focus our attention on *primitive* Teichmüller curves in \mathcal{M}_q : those that do not arise from lower genus.

To define these, let us say (X, ω) is the *pullback* of (Y, η) if there is a holomorphic map $f: X \to Y$ such that $\omega = f^*(\eta)$. A 1-form with g(X) > 1 is *primitive* if it is not the pullback of a form of lower genus.

Every form in $\Omega \mathcal{M}_g$, g > 1, is the pullback of a unique primitive 1-form (X, ω) [Mo1, Thm. 2.6], [Mc3, Thm. 2.1]. We say a Teichmüller curve is *primitive* if it is generated by a primitive 1-form. In this case $\operatorname{Aut}(X, \omega)$ is trivial, and hence

$$\operatorname{Aff}^+(X,\omega) \cong \operatorname{SL}(X,\omega).$$

Invariants. We conclude this section by discussing three invariants of the Teichmüller curve $f: V \to \mathcal{M}_g$ generated by a 1-form (X, ω) .

- 1. The lattice $SL(X, \omega)$, often called the *Veech group*, is determined by V up to conjugacy in $SL_2(\mathbb{R})$. Indeed, it is simply the Fuchsian group uniformizing V.
 - 2. The trace field of $SL(X,\omega)$, defined by

$$K = \mathbb{Q}(\operatorname{tr} A : A \in \operatorname{SL}(X, \omega)) \subset \mathbb{R},$$

is also an invariant of V. It is a totally real number field, of degree at most g over \mathbb{Q} , satisfying

$$(2.9) K = \mathbb{Q}(\operatorname{tr} A)$$

for any hyperbolic element $A \in \mathrm{SL}(X,\omega)$. Moreover $K = \mathbb{Q}$ if and only if (X,ω) is the pullback of a form of genus one.

3. All generators of V lie in the same stratum $\Omega \mathcal{M}_g(p)$, so this too is an invariant of V.

The trace field and stratum are known for all the Teichmüller curves V we will discuss below. The lattice $\mathrm{SL}(X,\omega)$, on the other hand, is often inaccessible. Nevertheless, topological invariants of V, such as its Euler characteristic, can frequently be determined.

3. Billiards

We now turn to the remarkable connection between Teichmüller curves and billiards in polygons.

The first nontrivial Teichmüller curves $V \subset \mathcal{M}_g$ were discovered in 1989 by Veech. They play a key role in his proof of:

Theorem 3.1. Billiards in a regular polygon P has optimal dynamics.

Here optimal dynamics means that any unit speed billiard trajectory $\tau : \mathbb{R} \to P$ satisfies the Veech dichotomy; it is either

- (i) periodic: meaning $\tau(t) = \tau(t+T)$ for some T>0; or
- (ii) uniformly distributed: meaning $\tau(\mathbb{R})$ is dense, and

$$\lim_{T \to \infty} \frac{1}{T} \int_0^T f(\tau(t)) \, dt = \frac{1}{\operatorname{area}(P)} \int_P f(z) \, |dz|^2$$

for any continuous function $f: P \to \mathbb{R}$.

Which alternative holds—(i) or (ii) above—depends only on the *initial slope* of the trajectory. See Figure 3.1 for examples.

In this section we describe the series of Teichmüller curves associated to regular polygons, and present the proof of Theorem 3.1, following [V1] and [Mas2]. We also summarize, in Theorem 3.9, the known examples of triangles with optimal billiards.

A striking feature of Theorem 3.1 is that it describes the behavior of every trajectory in P, and shows that only two, radically different types of behavior are

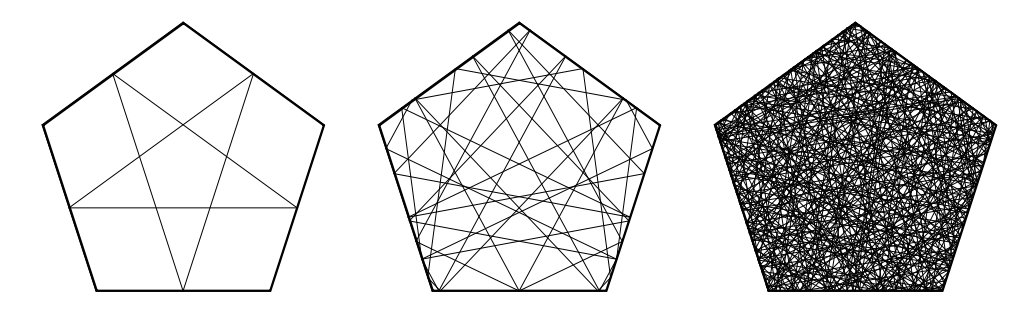


FIGURE 3.1. Three billiard trajectories in a regular pentagon.

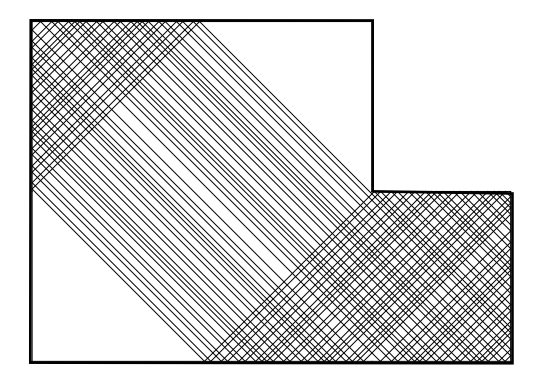


FIGURE 3.2. A billiard trajectory that is neither periodic nor dense.

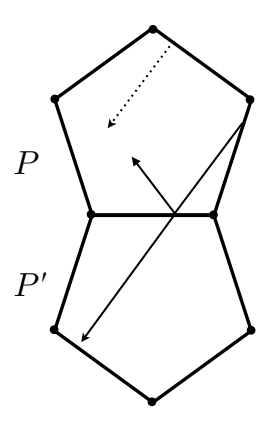


FIGURE 3.3. The double pentagon $P \cup P'$ yields a surface of genus 2.

possible. For more general polygons, some trajectories may be neither periodic nor dense (see Figure 3.2), and even dense trajectories may be unevenly distributed.

Unfolding. A polygon is *rational* if its angles lie in $\pi\mathbb{Q}$. To relate billiards to Teichmüller theory, we first explain how a rational polygon $P \subset \mathbb{C}$ determines a holomorphic 1-form $(X, \omega)_P$.

Suppose P is a regular pentagon. The construction of (X, ω) is described in Figure 3.3. The idea is that, when a billiard trajectory τ strikes an edge of P, rather than reflecting τ , we can reflect P. The result is an adjacent polygon P', and τ continues into P' along a straight line.

Now when τ strikes an edge of P', we could add yet another polygon P''; but P'' would simply be a translate of P. So instead of adding new polygons, we glue the edges of P' to parallel edges of P. Since $P \cup P'$ is combinatorially an octagon, the result is a 1-form

$$(X,\omega) = (P \cup P', dz)/\sim$$

of genus two; and billiard trajectories in P go over to geodesics on the flat surface $(X, |\omega|)$.

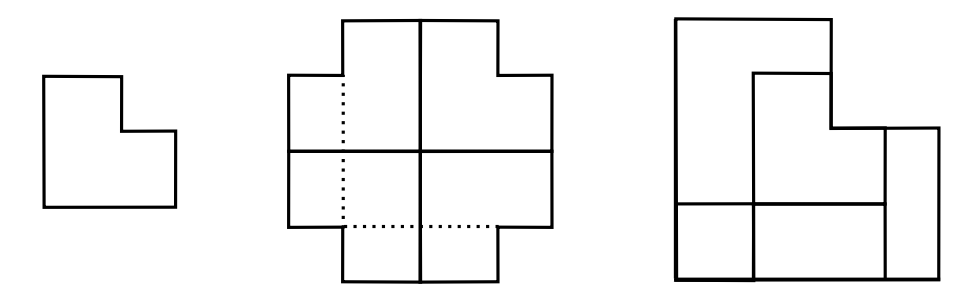


FIGURE 3.4. Unfolding an L-shaped polygon.

A similar construction can be carried out for any rational polygon P. The rationality condition means the group $G \subset O_2(\mathbb{R})$ generated by reflections in the sides of P is finite. Let H be the subgroup that stabilizes P up to translation. The associated 1-form is then given by

(3.1)
$$(X,\omega)_P = \left(\bigsqcup_{[g] \in G/H} (gP, dz) \right) / \sim .$$

Two examples. (i) If P is a regular 2n-gon, then $(X, \omega)_P$ is simply (P, dz) with opposite edges identified.

(ii) The polygon P = L(a, a) unfolds to give a Swiss cross with its sides identified; the resulting form $(X, \omega)_P$ is isomorphic to $L(a, a)/\sim$ up to a factor of two (see Figure 3.4).

From billiards to Teichmüller curves. We say P is a lattice polygon if $SL(X, \omega)_P$ is a lattice in $SL_2(\mathbb{R})$; equivalently, if $(X, \omega)_P$ generates a Teichmüller curve V. For brevity, we also say P generates V. The connection between billiards and Teichmüller curves is summed up by the following general statement.

Theorem 3.2. The billiard flow in a lattice polygon P has optimal dynamics.

With this result in hand, Theorem 3.1 follows from:

Theorem 3.3. Every regular polygon P generates a primitive Teichmüller curve. In particular, P is a lattice polygon.

Corollary 3.4. Every moduli space \mathcal{M}_g , g > 0, contains a primitive Teichmüller curve.

The invariants of these first examples of primitive Teichmüller curves are listed in Table 3.1. Note that $SL(X,\omega)_P$ is always a triangle group, that ω has just one or two zeros, and that every g occurs.

We will sketch the proof of Theorem 3.2 at the end of this section.

Algebraic models. One of the remarkable properties of a regular polygon P is that we have an explicit $algebraic\ model$ for the Teichmüller curve

$$f:V\to\mathcal{M}_g$$

it generates, to complement the *flat model* coming from the $SL_2(\mathbb{R})$ orbit of its unfolding. Recall that $T_n(x)$ denotes the degree n Chebyshev polynomial (see equation (1.1)).

Table 3.1. Invariants of Teichmüller curves generated by n-sided regular polygons.

Sides	Stratum	$\mathrm{SL}(X,\omega)$	Trace field
n = 2g + 1	$\Omega \mathcal{M}_q(2g-2)$	$\Delta(2, n, \infty)$	$\mathbb{Q}(\cos(2\pi/n))$
n=4g	225 V $t_g(2g-2)$	$\Delta(n/2,\infty,\infty)$	
n = 4g + 2	$\Omega \mathcal{M}_g(g-1,g-1)$	$\Delta(n/2,\infty,\infty)$	

Theorem 3.5. For n = 2g + 1 odd, the Teichmüller curve generated by a regular n-gon is given by $f(t) = [X_t]$, where X_t is the hyperelliptic curve defined by

$$y^2 = T_n(x) - t,$$

and t ranges in the space

$$V = (\mathbb{P}^1 - \{t : t^2 = 1\})/(t \sim -t).$$

The curves X_t and X_{-t} are isomorphic, since $T_n(x)$ is odd, and thus f is well-defined on V

The limiting curve X_{∞} is defined by $y^2 = x^n - 1$. Indeed, the unfolding of P yields the 1-form $(X_{\infty}, dx/y)$ generating V.

To take into account the symmetries of X_0 and X_∞ , we regard V as the $(2, n, \infty)$ orbifold; the unique cusp comes from $t = \pm 1$. Thus V is natural uniformized by $\Delta(2, n, \infty)$ as indicated in Table 3.1.

Even polygons. When n is even, a slightly different family is required. In this case $T_n(x)$ is also even, and we define X_t by the polynomial equation

$$y^2 = x(T_n(\sqrt{x}) - t)$$

for $t\in V=\mathbb{P}^1-\{t:t^2=1\}.$ The unfolding of P gives the form dx/y on the curve X_∞ defined by

$$y^2 = x(x^{n/2} - 1).$$

In brief, these formulas arise from the close relationship between the family of curves X_t , and the family of hyperelliptic curves Y_s branched over orbits $D_{2n} \cdot s$ of the dihedral group $D_{2n} \subset \operatorname{Aut} \mathbb{P}^1$.

The hidden symmetries of the pentagon. The fact that regular polygons generate Teichmüller curves (Theorem 3.3) can be verified by a direct calculation. To indicate the idea, we will show that

$$SL(X,\omega)_P = \Delta(5,2,\infty)$$

when P is a regular pentagon. (This group is conjugate to $\Delta(2,5,\infty)$.)

First, referring to Figure 3.3, observe that $\operatorname{Aut}(X)$ contains a symmetry of order 2 that exchanges P and P', and a symmetry of order 5 that rotates each. Their product ϕ gives an element of order 10 in $\operatorname{SL}(X,\omega)_P$, namely

$$S = D\phi = \begin{pmatrix} \cos(\pi/5) & \sin(\pi/5) \\ -\sin(\pi/5) & \cos(\pi/5) \end{pmatrix}.$$

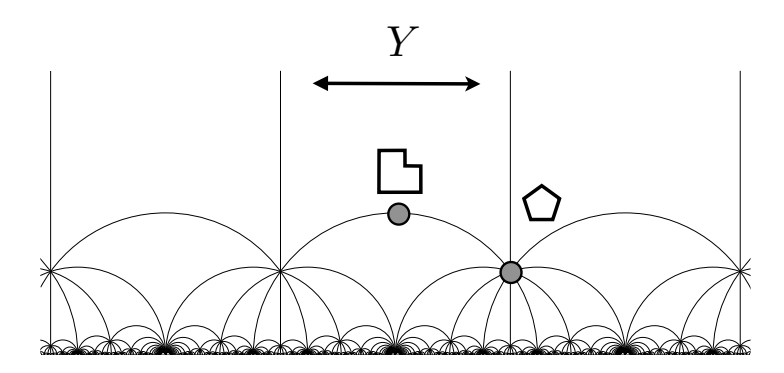


FIGURE 3.5. The Teichmüller curve $f: V = \mathbb{H}/\Delta(2,5,\infty) \to \mathcal{M}_2$ generated by the golden L and the regular pentagon P.

Second, observe that X decomposes into a pair of horizontal cylinders of equal modulus m. One of these cylinders is obtained by gluing the top two edges of P to the bottom two edges of P'; it is built from 2 isosceles triangles with angles $\pi(1,1,3)/5$. It follows readily that $m = \tan(\pi/5)/2$. Thus, by Proposition 2.3, the affine group of (X,ω) contains a product of Dehn twists τ with

$$T = D\tau = \begin{pmatrix} 1 & 2\cot(\pi/5) \\ 0 & 1 \end{pmatrix} \in SL(X, \omega)_P.$$

Noting that tr(ST) = 0, we find

$$\langle S, T \rangle = \Delta(5, 2, \infty) \subset \mathrm{SL}(X, \omega)_P$$

(see Appendix A). Since this triangle group is a lattice, so is $SL(X,\omega)_P$. (In fact equality holds above, since $\Delta(5,2,\infty)$ is a maximal discrete subgroup of $SL_2(\mathbb{R})$.) Its trace field $K=\mathbb{Q}(\sqrt{5})$ is quadratic, so the corresponding Teichmüller curve in \mathcal{M}_2 is primitive.

The golden table. Let $\gamma = (1 + \sqrt{5})/2 = 2\cos(\pi/5)$ denote the golden ratio. It can be shown by elementary geometry that the polygon $L = L(\gamma, \gamma)$ and the regular pentagon P generate the same Teichmüller curve. In fact, L corresponds to the orbifold point of order 2 on V, while P corresponds to the point of order 5 (see Figure 3.5). As an alternative to the calculation above, one can readily check that $\mathrm{SL}(X,\omega)_L = \Delta(2,5,\infty)$, using the fact that $(X,\omega)_L$ decomposes into 2 horizontal cylinders of modulus $1/\gamma$. (The similar case of L(2,2) was discussed in §2.)

Aside: Is the Veech dichotomy effective? Although Theorem 3.2 clearly separates the slopes in a lattice polygon P into two classes, it is an open problem to distinguish between them, even in the case of a regular polygon.

To make this precise, let $P_n \subset \mathbb{C}$ be a regular n-sided polygon resting on the real axis, let $S_n \subset \mathbb{R}$ be its set of periodic slopes, and let L(s) be the maximum number of times that a trajectory with slope $s \in S_n$ hits the sides of P_n before returning to its starting point.

It is easy to see that $S_n \subset K_n t_n$, where $K_n = \mathbb{Q}(\cos(2\pi/n))$ and $t_n = \tan(2\pi/n)$. Equality holds when $\deg(K_n/\mathbb{Q}) \leq 2$, and in fact

$$\log L(st_n) = O(h(s)^2),$$

where h(s) denotes the height of s [Mc10]. Otherwise, $S_n \neq K_n t$ [AS], and one can ask:

Question 3.6. Is there an algorithm to determine, given $s \in K_n$, if a trajectory with slope st_n in P_n is periodic?

Equivalently:

Question 3.7. Is there a computable function F such that $L(st_n) \leq F(s)$ whenever st_n is a periodic slope?

The first open case occurs when n = 7. In this case, an unexpected phenomenon arises: experimentally, many slopes that are *not* periodic are fixed by *hyperbolic* elements in the Veech group.

Question 3.8. Is every point $x \in \mathbb{Q}(\cos(\pi/7))$ the fixed point of a parabolic or hyperbolic element of $\Delta(2,7,\infty)$?

A positive answer would yield an algorithm for recognizing the periodic slopes in the heptagon.

Lattice triangles. For a more systematic enumeration of lattice polygons, it is natural to start with triangles.

To summarize what is known, let us say a triangle T has $type\ (a_1, a_2, a_3)$ if its internal angles are proportional to the integers $a_i \geq 1$. The type of T determines T up to similarity.

Theorem 3.9. Triangles of the following types generate Teichmüller curves:

```
A. (1,1,n), (2,n,n) and (2,n,n+2), n \ge 1;
```

B. (1,2,n), n > 5 odd;

C. (2,3,4), (3,4,5) and (3,5,7); and

D. (1,4,7).

Any other lattice triangle must be scalene and obtuse, like examples B and D above.

Corollary 3.10. All acute, right-angled, and isosceles lattice triangles are known.

Series A, discovered by Veech, produces the same Teichmüller curves as the regular polygons. Series B, discovered by Vorobets and studied by Ward, is genuinely new. These two series are special cases of the Bouw-Möller examples, to be discussed in §7. The three triangles in series C, discovered by Vorobets, Veech and Kenyon-Smillie, will be related to the exceptional Coxeter groups in §6. Example D, found by Hooper, generates a Teichmüller curve in the Weierstrass series $W_D \subset \mathcal{M}_4$ to be discussed in §5, namely W_{12} .

Question 3.11. Is the list of lattice triangles above complete?

Dynamics on moduli space. To conclude, we outline the proof of the Veech dichotomy, Theorem 3.2. The proof pivots on the following important result.

Theorem 3.12 (Masur). If the Teichmüller geodesic ray generated by (X, ω) is recurrent in \mathcal{M}_q , then every horizontal geodesic in $(X, |\omega|)$ is uniformly distributed.

The ray in question, defined by equation (2.5), shrinks the horizontal geodesics on X. This process accelerates the horizontal geodesic flow; indeed, the special properties of lattice polygons can be traced to the role played by $SL(X, \omega)$ as a renormalization group for the dynamics of billiards in P.

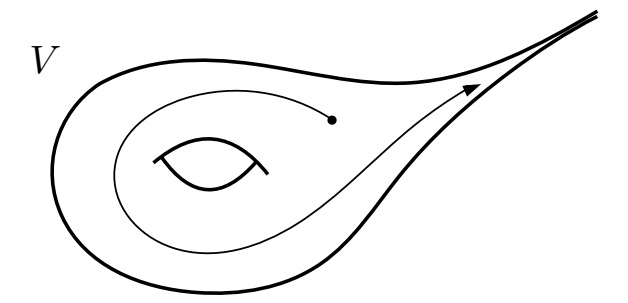


FIGURE 3.6. An escaping geodesic must converge to a cusp.

Sketch of the proof. Masur's original proof appears in [Mas2]; see also [Mc7]. Here we sketch a cohomological argument from [Mc8].

Let $P(\omega)$ be the cone of closed, positive de Rham currents carried by the foliation $\mathcal{F}(\omega)$ of X by horizontal geodesics. The long-term behavior of any horizontal geodesic is described by such a current. Using the Hodge norm on $H^1(X,\mathbb{R})$, one can measure the size of $P(\omega)$ by the diameter $d \leq 2$ of its intersection with the unit sphere.

Let $\gamma:[0,\infty)\to\mathcal{M}_g$ be the Teichmüller ray generated by (X,ω) . By contraction of the complementary period mapping, which records the Hodge structure on the part of $H^1(X,\mathbb{R})$ orthogonal to ω , every time the geodesic ray $\gamma(t)$ returns to a fixed compact set $K\subset\mathcal{M}_g$, one can improve the estimate on d by a factor of $\lambda_K<1$. Thus if γ is recurrent, we have d=0 and $P(\omega)$ reduces to the ray through Im ω . This means the horizontal foliation $\mathcal{F}(\omega)$ is uniquely ergodic, and hence every horizontal geodesic is uniformly distributed.

Proof of Theorem 3.2. Suppose P is a lattice polygon. Let

$$\gamma: [0,\infty) \to V = \mathbb{H}/\operatorname{SL}(X,\omega)_P \to \mathcal{M}_q$$

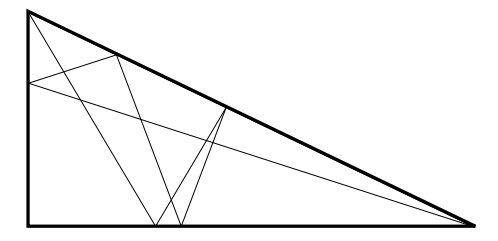
be the Teichmüller geodesic generated by $(X, \omega)_P$.

The Veech dichotomy reflects the following alternative for the behavior of a geodesic ray on a finite-volume hyperbolic surface such as V: either γ is recurrent, or γ converges to a cusp (see Figure 3.6). Recurrence implies every horizontal geodesic on (X,ω) is uniformly distributed, by Theorem 3.12; while convergence to a cusp implies every horizontal geodesic is periodic, by Proposition 2.3. Consequently, billiard trajectories in P with initial slope zero are either periodic or uniformly distributed as well. The same reasoning applies to other slopes, by rotating ω . \square

Remark: Billiards that hit vertices. The proof of the Veech dichotomy also shows that any infinite billiard trajectory starting at a vertex of P is uniformly distributed. However, a trajectory that joins a pair of vertices need not have periodic slope. A counterexample in the (2,5,7) lattice triangle is shown in Figure 3.7: the first trajectory joins a pair of vertices, while the second, parallel trajectory is aperiodic (cf. [Bo]).

Question 3.13. Must every edge of a lattice polygon have periodic slope?

A positive answer for quadratic trace fields is given in [Mc10, Cor. 6.3].



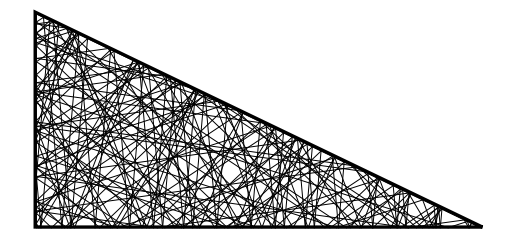


FIGURE 3.7. A billiard path joining two vertices need not have periodic slope; the parallel trajectory at the left is aperiodic.

4. Genus 2

The regular polygons provide only three examples of Teichmüller curves in \mathcal{M}_g for g=2: those generated by the regular pentagon, octagon and decagon.

It is thus natural to ask: are there infinitely many primitive Teichmüller curves $V \subset \mathcal{M}_2$? In this section we will see the answer is *yes*. In fact, we will present a complete classification of such curves, following the development in [Mc1] and its sequels. These curves were also discovered, from another perspective, in [Ca].

Real multiplication. Where should one look for Teichmüller curves $V \subset \mathcal{M}_g$?

It turns out that membership in V is reflected, not by the automorphism group of X, but by the *endomorphism ring* of its Jacobian.

To describe this connection, recall that the *Jacobian* of $X \in \mathcal{M}_g$ is the compact complex torus

$$\operatorname{Jac}(X) = \Omega(X)^*/H_1(X,\mathbb{Z}) \cong \mathbb{C}^g/L.$$

An endomorphism $T : Jac(X) \to Jac(X)$ is a holomorphic group homomorphism; it is self-adjoint if its action on $H_1(X, \mathbb{Z})$ satisfies

$$[T(C_1), C_2] = [C_1, T(C_2)]$$

with respect to the symplectic intersection pairing on 1-cycles. Equivalently, the action of T^* on $\Omega(X) \cong \Omega(\operatorname{Jac}(X))$ is self-adjoint for the inner product

$$\langle \omega_1, \omega_2 \rangle = \frac{i}{2} \int_X \omega_1 \wedge \overline{\omega}_2.$$

Let K be a totally real number field of degree g over \mathbb{Q} . We say $\mathrm{Jac}(X)$ admits real multiplication by K if there is an inclusion

$$\iota: K \to \operatorname{End}(\operatorname{Jac}(X)) \otimes \mathbb{Q}$$

and every $T \in \iota(K)$ is self-adjoint. Then $\Omega(X)$ admits an orthonormal basis of eigenforms $(\omega_1, \ldots, \omega_q)$, satisfying $K \cdot \omega_i \subset \mathbb{C}\omega_i$ for each i.

Taking into account the integral structure, one can say more precisely that $\operatorname{Jac}(X)$ admits real multiplication by the *order* $\mathcal{O} \subset K$ characterized by

$$\iota(\mathcal{O}) = \iota(K) \cap \operatorname{End}(\operatorname{Jac}(X)).$$

The Weierstrass curves. Now suppose g = 2. Then K is a real quadratic field, and an order

$$\mathcal{O} = \mathcal{O}_D \cong \mathbb{Z}[x]/(x^2 + bx + c) \subset K = \mathbb{Q}(\sqrt{D})$$

is uniquely determined by its discriminant $D = b^2 - 4c$. Any integer with D > 0, D = 0 or $1 \mod 4$ can occur, provided D is not a square.

For each such D, the Weierstrass curve $W_D \subset \mathcal{M}_2$ is defined to be the locus of $X \in \mathcal{M}_2$ such that

- (i) $\operatorname{Jac}(X)$ admits real multiplication by \mathcal{O}_D , and
- (ii) one of its eigenforms ω has a double zero.

(This double zero lies at one of the six Weierstrass points of X, hence the terminology.)

The first condition implies that X lies on a surface in \mathcal{M}_2 , birational to the Hilbert modular surface

$$\mathfrak{X}_D = \mathbb{H} \times \mathbb{H} / \operatorname{SL}(\mathcal{O}_D \oplus \mathcal{O}_D^{\vee}).$$

(This surface describes the possibilities for $\operatorname{Jac}(X)$.) The additional requirement that ω has a double zero, rather than two simple zeros, reduces W_D to an algebraic curve.

Classification. We can now state the classification of primitive Teichmüller curves in genus two.

Theorem 4.1. Each component of W_D is a primitive Teichmüller curve.

Theorem 4.2. The curve W_D is irreducible unless $D \equiv 1 \mod 8$, in which case it has two components.

In the second case the components W_D^{ϵ} are distinguished by a *spin invariant* $\epsilon = 0$ or 1.

Theorem 4.3. Every Teichmüller curve in $\bigcup W_D$ is generated by billiards in an explicit L-shaped table.

For example, when D is even, W_D is generated by L(a, a+1), where $a = \sqrt{D/4}$.

Corollary 4.4. There are infinitely many primitive Teichmüller curves in \mathcal{M}_2 .

The oasis. When the infinite sequence of curves W_D was first discovered, it seemed like we might be standing on the edge of a jungle, with many more curves to be found in the larger stratum $\Omega \mathcal{M}_2(1,1)$. A fruitless computer search, however, began to suggest that we had stumbled upon, not a jungle, but an oasis in a vast desert. This perception is confirmed by:

Theorem 4.5. The regular decayon generates the only other primitive Teichmüller curve in \mathcal{M}_2 .

The proof will be sketched at the end of this section.

Classification and synthesis. Taken together, the above results give a classification of the primitive Teichmüller curves in genus 2, in the following sense: (i) there is an explicit construction of all examples (e.g. using L-shaped tables); and (ii) there are readily computable invariants (D, ϵ) that allow one to test when two constructions yield the same Teichmüller curve. For example, the regular pentagon and octagon generate W_5 and W_8 , respectively.

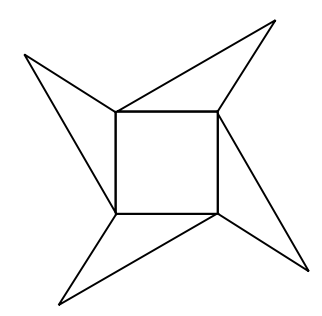


FIGURE 4.1. An orbifold point on W_D .

In contrast to the case of regular polygons, the definition of W_D is synthetic: it is an abstractly defined algebraic curve, whose properties remain to be investigated. There is no known general algebraic formula for W_D , although many particular cases have been treated. An understanding of the corresponding Veech groups is equally elusive.

Topology of W_D . Despite these mysteries, the following results provide a complete description of topology of W_D .

Theorem 4.6 (Bouw–Möller). If W_D has two components, they are homeomorphic as orbifolds.

Theorem 4.7 (Bainbridge). We have $\chi(W_D) = -(9/2)\chi(\mathfrak{X}_D)$.

The Euler characteristic of the Hilbert modular surface \mathfrak{X}_D defined by (4.1) is well–studied and related to the coefficients of a modular form. Writing $D = f^2 D_0$ where D_0 is a fundamental discriminant, it is given by

(4.2)
$$\chi(\mathfrak{X}_D) = 2f^3 \zeta_{\mathbb{Q}(\sqrt{D})}(-1) \left(\sum_{r|f} \left(\frac{D_0}{r} \right) \frac{\mu(r)}{r^2} \right).$$

(The summands involve the Jacobi symbol for (D_0, r) and the Möbius function $\mu(r)$.)

Theorem 4.8 (Mukamel). For D > 8, the orbifold points on W_D all have order 2. Their their total number $e_2(D)$ is a weighted sum of class numbers of the quadratic imaginary orders with discriminants -D, -4D and -D/4.

These orbifold points $X \in W_D$ can be described as octagonal pinwheels with their opposite sides identified (see Figure 4.1); they cover elliptic curves with complex multiplication, allowing one to give explicit equations for X. For example, the unique orbifold point $X \in W_{13}$ is defined by

$$y^2 = (x^2 - 1)(x^4 - ax^2 + 1),$$

where $a = 2594 + 720\sqrt{13}$.

There is a simple combinatorial method to enumerate the cusps of W_D . Combining these results, one can also compute the genus of its components. As a consequence, it is known that all components of W_D have genus $g \geq 1$ when D > 41, and that the genus grows roughly like $D^{3/2}$. Appendix C gives a table of invariants of $W_D \subset \mathcal{M}_2$ for all $D \leq 60$.

From affine maps to the Jacobian. Let us return to the definition of W_D , and sketch the proof of Theorem 4.1.

Where does real multiplication on $\operatorname{Jac}(X)$ come from? To answer this question, suppose $\operatorname{SL}(X,\omega)$ contains an element $A=D\phi$ with irrational trace $\lambda\in\mathbb{R}$. Here $\phi:X\to X$ is an affine automorphism. Since X has genus two, λ is quadratic over \mathbb{Q} ; we denote its Galois conjugate by λ' .

Typically, the action of A on $\mathbb{R}^2 \cong \mathbb{C}$ is only real linear. However, the transformation $A+A^{-1}=\lambda \cdot I$ is always complex linear. Thus the formally defined map

$$(4.3) T = \phi + \phi^{-1}$$

preserves the holomorphic form ω up to a constant factor; in fact, in view of equation (2.7) we have:

$$(4.4) T^*(\omega) = \phi^*(\omega) + (\phi^{-1})^*(\omega) = \lambda \omega.$$

To make rigorous sense of T, we first linearize ϕ by letting it act on $L = H_1(X, \mathbb{Z})$. Then equation (4.3) gives a well-defined endomorphism of T of L. Since ϕ preserves the intersection form, T is self-adjoint. Moreover, T immediately extends to an endomorphism of the real Lie group

$$(L \otimes \mathbb{R})/L \cong \operatorname{Jac}(X).$$

We claim the action of T on $\mathrm{Jac}(X)$ is holomorphic. To see this, consider the isomorphism

$$(4.5) \Omega(X) \cong H^1(X, \mathbb{R})$$

defined by $\eta \mapsto [\text{Re}(\eta)]$. Extend ω to an orthogonal basis (ω, ω') for $\Omega(X)$; then the splitting

$$\Omega(X) = \mathbb{C}\omega \oplus \mathbb{C}\omega'$$

corresponds, under the isomorphism (4.5), to the splitting

$$(4.6) H^1(X,\mathbb{R}) = S \oplus S^{\perp} = \operatorname{Re}(\mathbb{C}\omega) \oplus \operatorname{Re}(\mathbb{C}\omega').$$

Here S^{\perp} is defined using the (purely topological) intersection form on $H^1(X,\mathbb{R})$.

Since T^* preserves $H^1(X,\mathbb{Z})$, the multiplicaties of its eigenvalues λ and λ' must be the same. By equation (4.4), $T^*(S) = S$ and $T^*|S$ is multiplication by λ . Since T^* is self-adjoint, $T^*(S^{\perp}) = S^{\perp}$; and hence $T^*|S^{\perp}$ is multiplication by λ' . It follows that $T^*|\Omega(X)$ is a complex linear mapping, with eigenvectors ω and ω' , and hence T itself gives a holomorphic endomorphism of the Jacobian of X.

Summing up, we have shown:

Theorem 4.9. Suppose (X, ω) is a form of genus two and the trace field K of $SL(X, \omega)$ is quadratic. Then Jac(X) admits real multiplication by K, with ω as an eigenform.

The eigenform locus. For each discriminant D, define the eigenform locus in $\Omega \mathcal{M}_2$ by

$$\Omega E_D = \{(X, \omega) : w \text{ is an eigenform for real multiplication by } \mathcal{O}_D \}.$$

Theorem 4.9 shows that, if we are looking for forms that generate primitive Teichmüller curves, we can restrict attention to the 3-dimensional eigenform loci inside the 5-dimensional space $\Omega \mathcal{M}_2$. This fact motivates the definition of W_D .

Proof of Theorem 4.1. Using the splitting in equation (4.6), one can check that ΩE_D is $\mathrm{SL}_2(\mathbb{R})$ -invariant. Thus the same is true for the 2-dimensional variety

$$\Omega W_D = \Omega E_D \cap \Omega \mathcal{M}_2(2).$$

But the projection of this locus to \mathcal{M}_2 is exactly W_D . Thus each component V of W_D is a Teichmüller curve, generated by a form $(X, \omega) \in \Omega W_D$ lying above it; and V is primitive, because its trace field $\mathbb{Q}(\sqrt{D})$ is irrational.

Using Theorem 4.9, we obtain:

Corollary 4.10. If $(X, \omega) \in \Omega \mathcal{M}_2(2)$ and the trace field of $SL(X, \omega)$ is irrational, then $SL(X, \omega)$ is a lattice.

Taking into account Proposition 2.3 and Theorem 3.2, we also find:

Corollary 4.11. An L-shaped billiard table L(a,b) is a lattice polygon if and only if ab - a and ab - b are both rational.

For example, L(a,a) is a lattice polygon if and only if $a=(1+\sqrt{b})/2$ for some $b\in\mathbb{Q},\,b>1.$

Irreducibility: Computer-assisted proof. Next we indicate the proof of Theorem 4.2. Suppose for simplicity that D is even. We wish to show W_D is connected.

Let Γ_D denote the graph whose vertices correspond to the cusps of W_D , and whose edges join vertices that are related by a 'butterfly move'. The graph Γ_D is easily computed: its vertices correspond roughly to the L-shaped polygons that generate W_D , and its edges join cusps that are guaranteed, by an elementary argument, to lie in the same component.

To complete the proof, it suffices to show that Γ_D is connected for all even D. This is first verified computationally for all D < 2000. The remaining cases are handled using about 11,000 different connection strategies, related to the primes 3,5 and 7. These strategies are also generated and verified by computer, and shown to cover all cases.

The exceptional decagon. Finally, we describe the proof of Theorem 4.5: the regular decagon generates the only remaining primitive Teichmüller curve in \mathcal{M}_2 .

By construction, the Weierstrass curves have generators in $\Omega \mathcal{M}_2(2)$, and they account for all the primitive Teichmüller curves with generators in this stratum. Why does the larger stratum $\Omega \mathcal{M}_2(1,1)$ yield only one more example? The answer is contained in the following result, which applies to all $\Omega \mathcal{M}_q$.

Theorem 4.12 (Möller). Suppose $SL(X, \omega)$ is a lattice with trace field K. Then there is a surjective map from Jac(X) to a compatibly polarized Abelian variety A such that

- (1) ω corresponds to an eigenform for real multiplication by K on A; and
- (2) the difference of any two zeros of ω is torsion in A.

Corollary 4.13. If (X, ω) generates a primitive Teichmüller curve in \mathcal{M}_2 , and $Z(\omega) = \{p, q\}$, then p - q is torsion in Jac(X).

Equivalently, there is a meromorphic function f on X whose only zeros and poles are at p and q.

Sketch of the proof of Theorem 4.5. Let V be a primitive Teichmüller curve generated by $(X, \omega) \in \Omega \mathcal{M}_2(1, 1)$. By Theorem 4.9, $(X, \omega) \in \Omega E_D$ for some D.

Consider the closure of V in the compactified moduli space $\overline{\mathcal{M}_2}$. On the boundary, one obtains a stable 1-form (Y,η) with $Y \in \mathcal{M}_{0,4}$ and $\operatorname{Jac}(Y) \cong (\mathbb{C}^*)^2$. The real multiplication and torsion conditions persist in the limit, and give a pair of rational numbers α, β such that $\sin(\pi \alpha)/\sin(\pi \beta) \in \mathbb{Q}(\sqrt{D})$. The are 15 possible values for (α, β) . The pair (1/5, 2/5) gives rise the to regular decagon, and the remaining 14 values are ruled out by a computer–assisted calculation.

What is the shape of W_D ? Perhaps the main open question concerning Teichmüller curves in genus two is the structure of their Veech groups. It is remarkable that results like Corollary 4.10 allow one to certify that $SL(X,\omega)$ is a lattice, without even revealing the volume of its quotient. We conclude by stating:

Problem 4.14. Give a direct construction of the Veech groups of the Weierstrass curves $W_D \subset \mathcal{M}_2$.

Remark: Square discriminant. One can also define Weierstrass curves W_{d^2} for square discriminant, by replacing K with $\mathbb{Q} \oplus \mathbb{Q}$. The corresponding Teichmüller curves are not primitive, but many results (such as Theorem 4.2) naturally generalize to this case.

5. Genus 3 and 4

In this section we will use *Prym varieties*, which are variants of the Jacobian, to construct infinitely many primitive Teichmüller curves in genus 3 and 4, following [Mc3].

Eigenforms in higher genus. One natural approach to generalizing the construction of $W_D \subset \mathcal{M}_2$ is to consider the locus of eigenforms for real multiplication in $\Omega \mathcal{M}_g$. Unfortunately, for g > 2, this locus is generally not $\mathrm{SL}_2(\mathbb{R})$ -invariant [Mc1, Thm. 7.5].

On the other hand, Theorem 4.12 shows that along a Teichmüller curve, one should only expect real multiplication on a factor of Jac(X). If we arrange that this factor is 2-dimensional, then the arguments from genus two will apply; and if, moreover, we require that ω has only one zero, then the torsion condition in Theorem 4.12 will be vacuously satisfied.

The Weierstrass curves $W_D \subset \mathcal{M}_g$. These considerations motivate the following definition. Fix $g \geq 2$, and let D > 0 be a real quadratic discriminant. The Weierstrass locus $\Omega W_D \subset \Omega \mathcal{M}_g$ consists of those (X, ω) such that:

- (1) the form ω has a single zero, of multiplicity 2g-2;
- (2) there exists a (unique) involution $\rho \in \operatorname{Aut}(X)$ such that $\rho^*(\omega) = -\omega$;
- (3) the genus of X/ρ is g-2; and
- (4) the differential ω is an eigenform for real multiplication by \mathcal{O}_D on the Prym variety

$$\operatorname{Prym}(X,\rho) = (\Omega(X)^{-})^{*}/H_{1}(X,\mathbb{Z})^{-}.$$

The Prym variety is the polarized Abelian subvariety of $\operatorname{Jac}(X)$ corresponding to the (-1)-eigenspace of $\rho|\Omega(X)$. In the case above, it is 2-dimensional by the condition that $g(X/\rho) = \dim \Omega(X)^+ = g - 2$.

The Weierstrass curve $W_D \subset \mathcal{M}_g$ is the projection of ΩW_D to \mathcal{M}_g . It is sometimes denoted by $W_D(2g-2)$ to emphasize the fact that $(X,\omega) \in \Omega W_D(2g-2)$. By arguments similar to those for genus 2, we find:

Theorem 5.1. For any g and D, the Weierstrass curve $W_D \subset \mathcal{M}_g$ is a finite union of primitive Teichmüller curves.

Genus 2, 3 and 4. For g=2, ρ is the hyperelliptic involution on X, so we recover the definition of W_D from §4. As we will see in §6, it is straightforward to give explicit examples of forms in ΩW_D for g=3 and 4, and thereby establish:

Corollary 5.2. There are infinitely many primitive Teichmüller curves in \mathcal{M}_3 and \mathcal{M}_4 .

However, W_D is empty for $g \ge 5$. For example, when g = 5, the map $X \to X/\rho$ must be a covering map, contradicting the fact that ρ fixes the unique zero of ω .

Classification. The analogue of Theorem 4.2 in higher genus is:

Theorem 5.3 (Lanneau–Nguyen). For genus 3, W_D is irreducible if D is even; it has two components if $D \equiv 1 \mod 8$; and otherwise, it is empty.

For genus 4, W_D is irreducible for all D.

Near completeness in genus 3. In genus three, only three additional primitive Teichmüller curves are known.

Problem 5.4. Do the regular polygons with 7 and 14 sides, and the (2,3,4) triangle, generate all the primitive Teichmüller curves in genus 3 outside the Weierstrass series W_D ?

Although this problem remains open, the works of several authors, including Aulicino, Nguyen and Wright, combine to yield notable progress.

Theorem 5.5. The Weierstrass curves W_D account for all but finitely many primitive Teichmüller curves in genus 3.

The proof is sketched in §10.

As we will see in §9, the situation is surprisingly different in genus 4: two additional infinite families of primitive Teichmüller curves are now known. We remark that the (1, 4, 7) triangle (from §3) generates the curve $W_{12} \subset \mathcal{M}_4$.

Topology of the Weierstrass curves. Write $D = f^2 D_0$ where D_0 is a fundamental discriminant, and let $\xi(D) = 1$ if f is odd and 3/2 if f is even. Let $e_n(V)$ denote the number of orbifold points of order n on V.

The next three results, on components, Euler characteristic and orbifold points, lead to a complete description of the topology of W_D in genus 3 and 4.

Theorem 5.6 (Zachhuber). In genus 3, whenever W_D has two components they are homeomorphic orbifolds.

Theorem 5.7 (Möller). In genus 3, each component V of W_D satisfies

$$\chi(V) = (-5/2)\xi(D)\chi(\mathfrak{X}_D).$$

In genus 4, we have $\chi(W_D) = -7\chi(\mathfrak{X}_D)$.

Theorem 5.8 (Torres–Zachhuber). We have $e_4(W_8) = e_6(W_{12}) = 1$ in genus 3, and $e_5(W_5) = e_6(W_{12}) = 1$ in genus 4. Otherwise, only orbifold points of orders n = 2 and 3 occur, and $e_n(W_D)$ can be calculated by elementary means for both g = 3 and g = 4.

For example, in genus 3, if D > 12 is an even fundamental discriminant, then

$$e_2(W_D) = |\{(a, b, c) \in \mathbb{Z}^3 : a^2 + b^2 + c^2 = D \text{ and } \gcd(a, b, c) = 1\}|/24.$$

There is also a combinatorial method to enumerate the cusps of W_D , used in the proof of Theorem 5.3, and thus the genus (of its components) can be routinely computed as well. Appendix C gives a table of these invariants of W_D for $D \leq 60$ and g = 2, 3 and 4.

Comparison to genus 2. The strategy for proving the results above is similar to the case g=2; for example, Theorem 5.3 is established via a computer–assisted study of elementary moves connecting cusps of W_D . However several new challenges arise in higher genus. For example, when g=3, a new invariant is required to distinguish the components of W_D , $D\equiv 1 \mod 8$; the Prym variety is not principally polarized, leading to the factor of $\xi(D)$ in Theorem 5.7; and the combinatorial complexities grow substantially as g increases.

6. Multicurves and Coxeter diagrams

In this section we turn to topology, to address the following question:

How can one describe a Teichmüller curve by a finite amount of combinatorial data?

We will see that one such description is provided by a weighted system of simple closed curves (A, B, m) on a topological surface Σ_q of genus g.

The intersection pattern between A and B is recorded by a Coxeter diagram $\Gamma(A,B)$. As observed by Leininger, the spherical diagrams give rise to Teichmüller curves. In particular, the exceptional spherical diagrams E_6 , E_7 and E_8 correspond to the sporadic lattice triangles from §3. We will also see that suitably chosen curve systems yield explicit examples of Weierstrass curves W_D in \mathcal{M}_g for g=2,3 and 4. Finally, curve systems whose Coxeter diagrams are grid graphs will play an important role in §7.

Multicurves. A multicurve $A \subset \Sigma_g$ is a union of disjoint, essential, simple closed curves, no two of which bound an annulus. A pair of multicurves (A, B) bind the surface Σ_g if they meet only in transverse double points, and each component of $\Sigma_g - (A \cup B)$ is a polygonal region with at least 4 sides (running alternately along A and B).

Index the components of A and B so that $A = \bigcup_{i=1}^{a} C_i$ and $B = \bigcup_{i=1}^{b} C_i$. We can then form the symmetric matrix

$$Q_{ij} = |C_i \cap C_j|,$$

with $Q_{ii} = 0$. It is convenient to record this matrix by a Coxeter diagram $\Gamma(A, B)$ with a + b vertices and Q_{ij} edges from vertex i to vertex j.

We say (A, B) is orientable if the curves C_i can be oriented so their algebraic intersection numbers satisfy $C_i \cdot C_j = Q_{ij}$ for all i < j.

Next, assign a positive integral weight m_i to each curve C_i (or equivalently, to each vertex of $\Gamma(A, B)$). Let

$$\mu = \mu(A, B, m) = \rho(m_i Q_{ij})$$

denote the spectral radius of the matrix on the right. Let τ_i denote a right Dehn twist around C_i , and let

$$\tau_A = \tau_1^{m_1} \circ \cdots \circ \tau_a^{m_a}, \qquad \tau_B = \tau_{a+1}^{m_{a+1}} \circ \cdots \circ \tau_{a+b}^{m_{a+b}}.$$

We then have:

Theorem 6.1 (Thurston). An orientable curve system (A, B, m) canonically determines a holomorphic 1-form $(X, \omega) \in \Omega \mathcal{M}_g$, unique up to a real scale factor, such that the multitwists τ_A and τ_B are realized by affine automorphisms satisfying

$$D au_A = \begin{pmatrix} 1 & \mu \\ 0 & 1 \end{pmatrix}, \qquad D au_B = \begin{pmatrix} 1 & 0 \\ -\mu & 1 \end{pmatrix}.$$

The trace field of $SL(X, \omega)$ is given by $K = \mathbb{Q}(\mu^2)$, and (X, ω) inherits the symmetries of the data (A, B, m).

Sketch of the proof. By the Perron–Frobenius theorem, there is a positive eigenvector (h_i) , unique up to scale, such that

(6.1)
$$\mu h_i = m_i \sum_{1}^{a+b} Q_{ij} h_j.$$

Take one rectangle $R_p = [0, h_i] \times [0, h_j] \subset \mathbb{C}$ for each $p \in C_i \cap C_j$, i < j, and glue (R_p, dz) to (R_q, dz) whenever p and q are joined by an edge of the one–complex $\bigcup C_i = A \cup B$. The result is a holomorphic 1-form (X, ω) such that each C_i is represented by a horizontal or vertical cylinder of height h_i , circumference $c_i = \mu h_i/m_i$, and modulus m_i/μ . It follows that the twists $\tau_i^{m_i}|C_i$ fit together to give a pair of globally defined affine automorphisms, τ_A and τ_B , with the indicated derivatives. To compute the trace field, observe that $\operatorname{Tr} D(\tau_A \tau_B^{-1}) = 2 + \mu^2$ and apply equation (2.9).

Remarks.

- (1) The stratum $\Omega \mathcal{M}_g(p)$ containing (X, ω) can also be read off from the topological data (A, B): the zeros of ω of order p correspond to components of $\Sigma_g (A \cup B)$ with 4p + 4 sides.
- (2) Every Teichmüller curve V can be specified by a multicurve system (A, B, m). To see this, let (Y, η) be a generator of V, and let (A, B, m) be the multicurve system coming from two different cylinder compositions of Y and their moduli. The corresponding 1-form (X, ω) is then affinely isomorphic to (Y, η) , so it also generates V.
- (3) Conversely, if $\mu(A, B, m) \leq 2$, then (X, ω) generates a Teichmüller curve. Indeed, the finite volume region in \mathbb{H} defined by $|\operatorname{Re}(z)|, |\operatorname{Re}(1/z)| \leq \mu/2$ meets every orbit of the subgroup generated by $D\tau_A$ and $D\tau_B$, so these two elements already generate a lattice in $\operatorname{SL}_2(\mathbb{R})$.
- (4) The fact that μ is an eigenvalue of a real symmetric matrix shows that the trace field of any Teichmüller curve is totally real, as mentioned in §2.

Relation to Coxeter groups. Suppose $Q_{ij} \leq 1$ for all i, j; in other words, suppose that any pair of loops in the multicurve system meet at most once. Then the graph $\Gamma = \Gamma(A, B)$ is a traditional *Coxeter diagram*, describing a reflection group W acting on \mathbb{R}^C and preserving the quadratic form 2I - Q. This diagram is *spherical* if 2I - Q is positive–definite, or equivalently, if $\rho(Q) < 2$. In this case

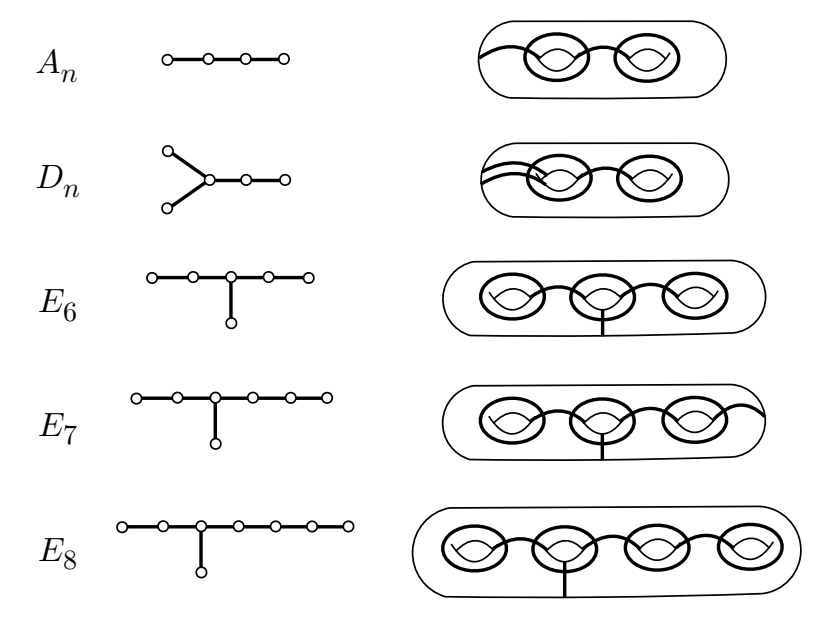


FIGURE 6.1. Spherical Coxeter diagrams and their corresponding curve systems.

 $\mu(A, B, I) < 2$, where I means we set all weights $m_i = 1$; so by Remark (3) above, we have:

Theorem 6.2 (Leininger). Whenever $\Gamma(A, B)$ is a spherical Coxeter diagram, the 1-form associated to (A, B, I) generates a Teichmüller curve V.

In brief, we say $\Gamma(A, B)$ generates V.

Regular polygons revisited. The (simply–laced) spherical Coxeter diagrams are well–known and shown in Figure 6.1, together with their corresponding curve systems (A, B) (which are uniquely determined).

Note that A_n and D_n are infinite series, and D_n violates our assumptions in a minor way, since it has two parallel curves. We have already seen the corresponding series of Teichmüller curves: they come from the regular polygons with k sides. In fact, D_n corresponds to k = 2n - 2, and A_n corresponds to k = n + 1. (When n is odd, the A_n form is not primitive, and a double covering also intervenes.)

The three sporadic Teichmüller curves. As Leininger shows, the exceptional diagrams are also related to billiards in the triangles listed in Theorem 3.9(C).

Theorem 6.3. The Coxeter diagrams E_6 , E_7 and E_8 generate the same Teichmüller curves as the three sporadic triangles. All three curves are primitive.

The invariants of these sporadic Teichmüller curves are summarized in Table 6.1. The notation Δ^- indicates that the Veech groups for E_7 and E_8 do not contain -I (see Appendix A); no other primitive Teichmüller curves are known with this property. The absence of -I can be traced to the asymmetry of the E_7 and E_8 diagrams.

Diagram Triangle $SL(X,\omega)$ Stratum Trace Field $\mathbb{Q}(\sqrt{3})$ E_6 (3, 4, 5) $\Delta(6,\infty,\infty)$ $\Omega_3(4)$ E_7 (2,3,4) $\Delta^{-}(9,\infty,\infty)$ $\Omega_3(1,3)$ $\mathbb{Q}(\cos \pi/9)$ E_8 (3, 5, 7) $\Delta^{-}(15,\infty,\infty)$ $\Omega_4(6)$ $\mathbb{Q}(\cos \pi/15)$

Table 6.1. The sporadic Teichmüller curves.

We note that the numbers 6,9 and 15, describing the Veech groups in Table 6.1, are simply half the Coxeter numbers h=12,18 and 30 for the corresponding diagrams.

It is also easy to give algebraic generators for the sporadic Teichmüller curves. In general, the unfolding $(X,\omega)_P$ of an (a,b,c) triangle gives, up to a complex factor, the 1-form

$$\omega = \frac{y \, dx}{x(x-1)}$$

on the curve X defined by

$$y^{a+b+c} = x^a(x-1)^b$$

(assuming gcd(a, b, c) = 1). For E_6 we obtain $y^{12} = x^3(x-1)^4$, and similarly for E_7 and E_8 .

Weierstrass curves in genus 3 and 4. To conclude, we will show how Coxeter diagrams can be used to construct explicit 1-forms generating infinitely many primitive Teichmüller curves $V \subset \mathcal{M}_g$ for g = 2, 3 and 4.

Let P be one of the three polygons shown in Figure 6.2. By gluing together parallel sides of P, we obtain a closed surface $Y = P/\sim$ of genus g = 2, 3 or 4, depending on the shape of P.

The surface Y decomposes into horizontal and vertical cylinders, which define a multicurve system (A, B) whose Coxeter diagram is shown below P. The numeric labels indicate the correspondence between the cylinders of Y and the vertices of $\Gamma(A, B)$.

Note that the L and S shaped polygons gives diagrams $\Gamma(A, B)$ isomorphic to A_4 and E_6 ; we will denote the final diagram by X_8 . Rotation of P through 180° gives an involution $\rho: Y \to Y$ inducing an automorphism of $\Gamma(A, B)$. A system of weights (m_i) on the vertices of $\Gamma(A, B)$ is symmetric if it is invariant under ρ . We can now state:

Theorem 6.4. Let m be a set of symmetric weights on the A_4 , E_6 or X_8 diagram, such that $\mu^2 = \mu(A, B, m)^2$ is quadratic over \mathbb{Q} . Then the corresponding 1-form (X, ω) generates a Teichmüller curve

$$V \subset W_D \subset \mathcal{M}_a$$

for some D, with trace field $K = \mathbb{Q}(\sqrt{D}) = \mathbb{Q}(\mu^2)$.

Proof. Due to the symmetry of m, there is an involution $\rho \in \operatorname{Aut}(X)$ such that $\rho^*(\omega) = -\omega$. It is readily verified that $g(X/\rho) = g(X) - 2$ and that ω has a unique zero. By Theorem 6.1, $\operatorname{SL}(X,\omega)$ has trace field K. A generalization of Theorem 4.9 then implies that ω is an eigenform for real multiplication by K on $\operatorname{Prym}(X,\rho)$, and hence $(X,\omega) \in \Omega W_D$ for some D as above.

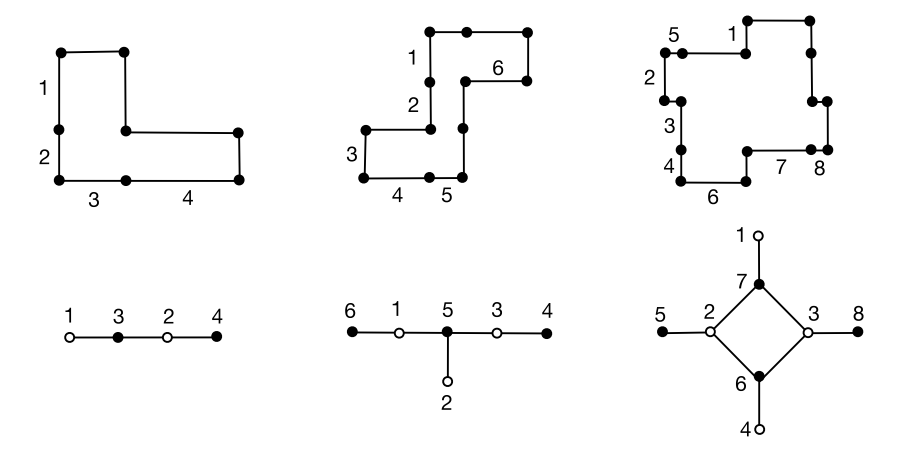


FIGURE 6.2. Polygons of shapes L, S and X yields surfaces of genus 2, 3 and 4.

Note that a solution to the eigenvalue equation (6.1) gives explicit lengths for the edges of P such that P/\sim generates a component of W_D . By varying the weights m, we obtain infinitely many fields K, and hence infinitely many Teichmüller curves in genus 2, 3 and 4.

Remark: Three views of the pentagon curve. As a particular case, we now have three different constructions of the Teichmüller curve $W_5 \subset \mathcal{M}_2$: it arises from the golden L-shaped table; from the regular pentagon; and from the A_4 Coxeter diagram.

7. Higher genus

In this section we describe the *Bouw-Möller series* of primitive Teichmüller curves $V_{pq} \subset \mathcal{M}_g$, indexed by pairs of integers $p,q \geq 2$ with $pq \geq 6$. We refer to V_{pq} as a *vertical series*, since $g \to \infty$ as $\max(p,q) \to \infty$. The curve V_{pq} depends only on the unordered pair (p,q); however each curve has two natural generators, $(X,\omega)_{pq}$ and $(X,\omega)_{qp}$.

For $g \geq 5$, the only know primitive Teichmüller curves in \mathcal{M}_g come from the Bouw–Möller series. The regular polygons, and the infinite series of lattice triangles of type (1,2,n) (see Theorem 3.9), correspond to V_{pq} with p=2 and p=3 respectively. We will see that every V_{pq} is generated by billiards in a generalized polygon T_{pq} , and that the corresponding Veech group is commensurable to a triangle group.

Semiregular polygons. The original approach of Bouw and Möller emphasized algebraic geometry. Here we will define V_{pq} using polygons, following Hooper. The two definitions coincide, as can be seen by comparing algebraic expressions for their generating 1-forms.

A semiregular polygon $R_q(a,b) \subset \mathbb{C}$ is a 2q-sided polygon, with equal internal angles, whose sides alternate in length between the values a and b. We also allow a or b to equal zero, in which case $R_q(a,b)$ becomes a regular q-sided polygon. A polygon is semiregular iff all its angles are equal, and its vertices lie on a circle.

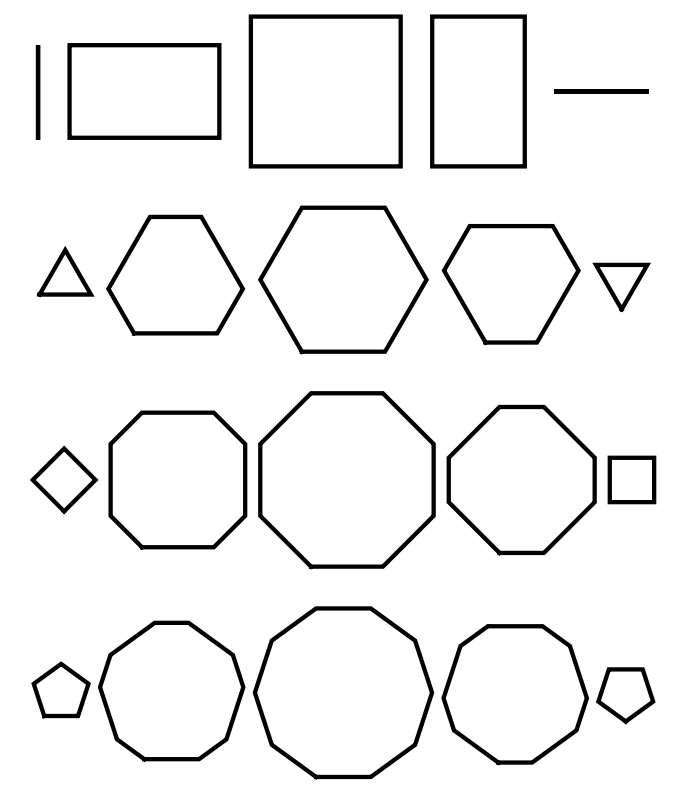


FIGURE 7.1. Each row shows the polygons used to construct $(X,\omega)_{5q},\ q=2,3,4,5.$ The top row gives $L(\gamma,\gamma)/\sim$.



FIGURE 7.2. For (p,q)=(8,4), only the first 4 polygons are used to construct $(X,\omega)_{pq}$.

Polygonal generators for V_{pq} . Let $p,q \geq 2$ be integers with $pq \geq 6$. The Teichmüller curve V_{pq} is generated by a form $(X,\omega)_{pq}$ constructed by gluing together a sequence of semiregular 2q-gons P_k , $k=1,2,\ldots,p$.

To define these, let $a_k = \sin(\pi k/p)$, k = 0, 1, ..., p. Let P_k be a copy of $R_q(a_{k-1}, a_k)$, for k = 1, 2, ..., p. Note that P_1 and P_p are regular polygons with q sides.

We aim to glue P_k to P_{k+1} for each k, so we rotate these polygons to make the corresponding sides of length a_k parallel. We then define

$$(X,\omega)_{pq} = \left(\bigsqcup_{k=1}^{p} '(P_k, dz) \right) / \sim .$$

The prime indicates that, as in the unfolding process (3.1), we identify P_k with P_ℓ if they are equal up to translation. Equivalently, if $p=q=0 \,\mathrm{mod}\, 2$, we only take the union from k=1 to p/2; otherwise, we take the union from k=1 to p. The form $(X,\omega)_{pq}$ is well-defined up to a complex multiple.

Let G_{pq} denote the (p,q) grid graph, whose vertices coincide with the integral points inside $[1, p-1] \times [1, q-1] \subset \mathbb{R}^2$, and whose edges connect points that are distance one apart.

Theorem 7.1 (Hooper). The forms $(X, \omega)_{pq}$ and $(X, \omega)_{qp}$ generate the same Teichmüller curve $V_{pq} \subset \mathcal{M}_g$.

The curve V_{pq} can also specified by a multicurve system (A, B, I) on Σ_g whose Coxeter diagram $\Gamma(A, B)$ is the grid graph G_{pq} .

Theorem 7.2 (Bouw–Möller). The Veech group of V_{pq} is commensurable to $\Delta(p, q, \infty)$, and V_{pq} is primitive provided $(p, q) \neq (6, 6)$.

A sketch of the proofs is deferred to the end of this section. See Theorem 7.6 for a more precise statement of Theorem 7.2.

Examples. The polygons (P_1, \ldots, P_p) are shown in several cases in Figure 7.1. Figure 7.2 illustrates an example where both p and q are even.

The Teichmüller curves generated by r-sided regular polygons coincide with V_{2r} . Indeed, $(X, \omega)_{2r}$ is just the usual unfolding of a regular r-gon. On the other hand, these curves are also generated by the forms $(X, \omega)_{r2}$, which are built out of rectangles. For example, the top row in Figure 7.1 gives the form $L(\gamma, \gamma)/\sim$ which, as we have seen in §3, generates the same curve as the regular pentagon.

Algebraic generators. We now turn an algebraic description of $(X, \omega)_{pq}$. Recall that $T_m(x)$ denotes the Chebyshev polynomial of degree m, characterized by equation (1.1). We let $\widetilde{T}_m(x)$ denote the unique polynomial satisfying

$$T_{2m+1}(x) - 1 = \widetilde{T}_m(x)^2(x-1)$$

and having positive leading coefficient. Let

$$z = \begin{cases} T_m(x) & \text{if } p = 2m \text{ is even, and} \\ \widetilde{T}_m(x) & \text{if } p = 2m + 1 \text{ is odd.} \end{cases}$$

Theorem 7.3. The form $(X, \omega)_{pq}$ is given by

$$\omega = \frac{y \, dx}{z(x-1)}$$

on the curve X defined by

$$y^{2q}=z^2(x-1)$$
 if p is odd,
 $y^{2q}=z^2(x-1)^q$ if p is even and q is odd, and
 $y^q=z(x-1)^{q/2}$ if both p and q are even.

Note that the automorphism $y \mapsto -y$ shows that $-I \in \mathrm{SL}(X,\omega)_{pq}$ for all p and q. Observing that the zeros of ω lie over $x = \infty$, we obtain:

Corollary 7.4. The form $(X, \omega)_{pq}$ lies in the stratum $\Omega \mathcal{M}_g(a^b)$, where

$$b = \gcd(p, q)$$
 and $a = \frac{pq - p - q}{b} - 1$



FIGURE 7.3. Construction of the billiard table T_{54} .

if p or q is odd, and

$$b = \frac{\gcd(p+q, p-q)}{2} \quad and \quad a = \frac{pq-p-q}{2b} - 1$$

if both p and q are even. In either case, 2q - 2 = ab.

Billiards. Let us say a polygon P has type (a_1, \ldots, a_n) if its internal angles, in order, are proportional to these values. By inspecting the algebraic formulas for $(X, \omega)_{pq}$, we also obtain:

Corollary 7.5. The form $(X, \omega)_{pq}$ is the unfolding of a generalized polygon T_{pq} of type

$$(a_1, \dots, a_n) = \begin{cases} (q, 2, 2, \dots, 2, pq - p - q) & \text{when } p \text{ is even, and} \\ (1, 2, 2, \dots, 2, pq - p - q) & \text{when } p \text{ is odd,} \end{cases}$$

where $n = 2 + \lfloor p/2 \rfloor$. The billiard flow in T_{pq} has optimal dynamics.

Example. The quadrilateral T_{54} , of type (1, 2, 2, 11), can be assembled from four pie-slices taken out of the semiregular polygons (P_1, \ldots, P_5) ; see Figure 7.3. This construction is used in the proof of both Theorem 7.3 and its Corollary 7.4 above.

Generalized polygons. Let us now explain the statement of Corollary 7.5 for general (p,q) in more detail.

The explicit formulas in Theorem 7.3 allow one to regard ω as a multi-valued form on the Riemann sphere with coordinate x; for example, when p=2m+1 is odd, we have

$$\omega = (x-1)^{1/2q-1} \prod_{i=1}^{m} (x-b_i)^{1/q-1} dx,$$

where b_1, \ldots, b_m are the roots of $\widetilde{T}_m(x)$. Since the roots b_i are real, we can choose a single-valued branch of ω on \mathbb{H} .

Intrinsically, we can regard

$$T_{pq} = (\overline{\mathbb{H}}, |\omega|)$$

as an abstract compact surface, with a flat Riemannian metric and piecewise—geodesic boundary. Topologically, T_{pq} is a disk; metrically, it can be constructed by gluing together finitely many Euclidean triangles.

We refer to any such metrized disk as a generalized polygon. By solving the equation $df = \omega$ on \mathbb{H} , we obtain a locally isometric developing map

$$f:T_{pq}\to\mathbb{C}.$$

Since $f^*(dz) = \omega$, we can regard $(X, \omega)_{pq}$ as the unfolding of T_{pq} . Geodesics reflecting off the boundary define a billiard flow in T_{pq} , which has optimal dynamics by a generalization of Theorem 3.2.

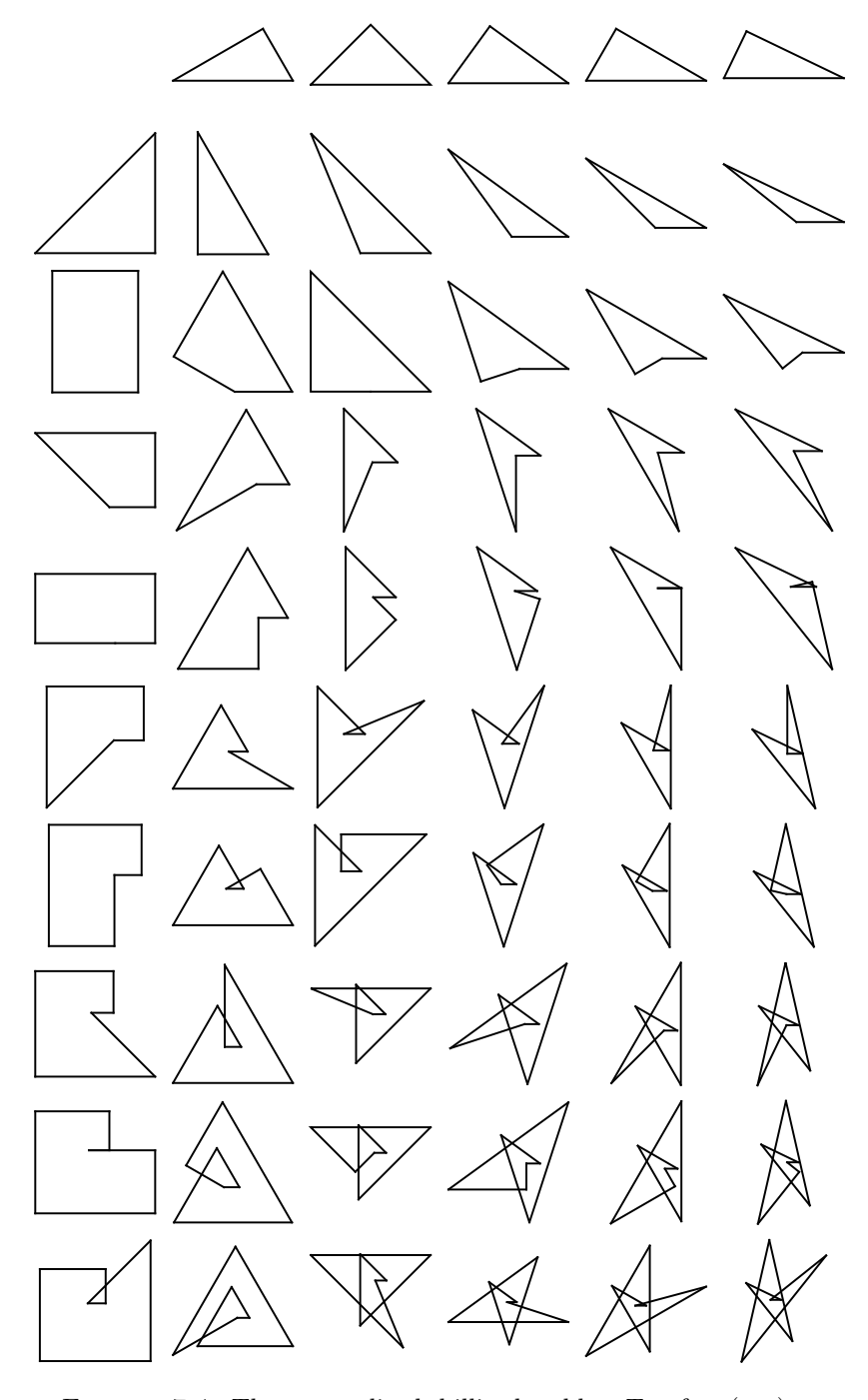


FIGURE 7.4. The generalized billiard tables T_{pq} for $(p,q) \in [2,11] \times [2,7].$

Now if f is injective, the expression $f(x) = \int \omega(x) dx$ is simply an instance of the Schwarz-Christoffel formula. Thus its image $f(\overline{\mathbb{H}}) \subset \mathbb{C}$ is a polygon isometric to T_{pq} . In general, $f|\mathbb{H}$ is only locally injective; but in either case, the exponents appearing in the formula for ω in Theorem 7.3, determine the internal angles of T_{pq} , yielding Corollary 7.5.

A sampler. One can visualize T_{pq} as an immersed polygon by drawing the image of its boundary under the developing map; see Figure 7.4. We emphasize that T_{pq} and T_{qp} both generate V_{pq} . For example, the first row in Figure 7.4 generates the same Teichmüller curves as the regular polygons; the same is true of the first column.

The generalized billiard table T_{pq} for (p,q)=(60,40) is shown in Figure 1.2.

Three—dimensional billiards. One can imagine an immersed polygon as describing a traditional billiard table not in 2 dimensions, but in 3: a table that is nearly flat, but with some parts of table passing above or below other parts.

The Veech group. The following more precise version of Theorem 7.2 completes our description of the Bouw–Möller series.

Theorem 7.6. Provided g > 1, the Veech group of $V_{pq} \subset \mathcal{M}_q$ is given by

$$\mathrm{SL}(X,\omega)_{pq} \cong \begin{cases} \Delta(p,q,\infty) & \text{if } p \neq q \text{ and } p \text{ or } q \text{ is odd;} \\ \widetilde{\Delta}(p/2,q/2,\infty,\infty) & \text{if } p \neq q \text{ and both are even;} \\ \Delta(2,p,\infty) & \text{if } p = q \text{ is odd; and} \\ \Delta(p/2,\infty,\infty) & \text{if } p = q \text{ is even.} \end{cases}$$

The trace field of V_{pq} is the same as the invariant trace field of $\Delta(p,q,\infty)$, which is given in Appendix A. Invariants of the Bouw-Möller curves in \mathcal{M}_g for g=2,3,4,5 and 6 are tabulated in Appendix D

Sketch of the proof of Theorems 7.1 and 7.2. We conclude by explaining why the forms constructed from biregular polygons generate Teichmüller curves.

Fix (p,q). We can assume that at least one of the polygons among (P_1,\ldots,P_p) has a horizontal edge, as in Figure 7.1. It is then straightforward to compute the cylinder decomposition of $(X,\omega)_{pq}$ at angles $\theta=0$ and $\theta=\pi/q$. The resulting multicurve system, of the form $(A,B,I)_{pq}$, uniquely determines the $\mathrm{SL}_2(\mathbb{R})$ orbit of $(X,\omega)_{pq}$.

It turns out that the associated Coxeter diagram $\Gamma(A,B) \cong G_{pq}$ is a rectangular grid, and the isomorphism $G_{pq} \cong G_{qp}$ is reflected by an isomorphism $(A,B,I)_{pq} \cong (A,B,I)_{qp}$. Thus reversing the roles of p and q does not change the $\mathrm{SL}_2(\mathbb{R})$ orbit of $(X,\omega)_{pq}$. In particular, we obtain an isomorphism

$$\iota : \mathrm{SL}(X, \omega)_{qp} \cong \mathrm{SL}(X, \omega)_{pq}.$$

Clearly, $\mathrm{SL}(X,\omega)_{pq}$ contains an element S_{pq} of order q, coming from the rotational symmetry of the polygons (P_1,\ldots,P_p) . Similarly, the isomorphism above provides an element $\iota(S_{qp}) \in \mathrm{SL}(X,\omega)_{pq}$ of order p. These two elements nearly generate the $\Delta(p,q,\infty)$ triangle group. A more precise analysis leads to Theorems 7.2 and 7.6.

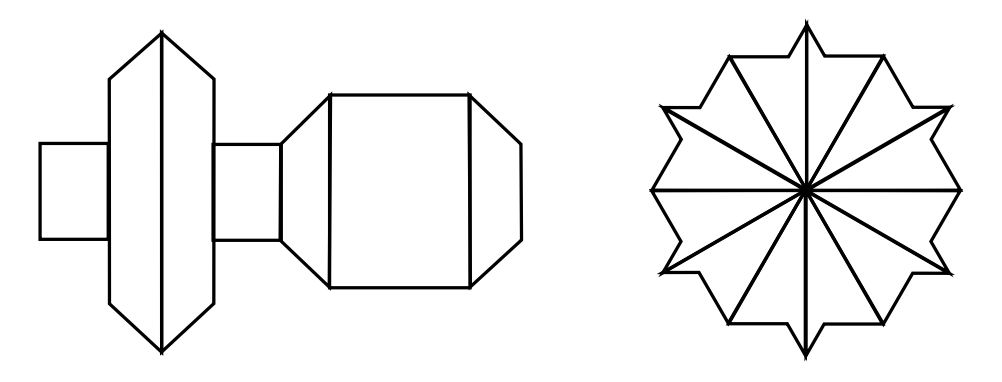


FIGURE 8.1. Polygonal models for forms in ΩG_D and ΩA_D .

8. Gothic curves and the flex locus

Do the horizontal Weierstrass series and the vertical Bouw–Möller series account for all the primitive Teichmüller curves (apart from a few sporadic examples)?

In this section we will see the answer is no. To do so, we will describe the sequence of gothic curves $G_D \subset \mathcal{M}_4$, and their relationship to the remarkable flex locus $F \subset \mathcal{M}_{1,3}$.

The flex locus gives the first example of a primitive Teichmüller surface, i.e. a totally geodesic variety of dimension two. The curves G_D and the surface F are intertwined by the algebraic geometry of cubic curves in the plane and space curves of genus four. This section follows the development by Mukamel, Wright and the author in [MMW].

In the next section we will present the last known family of primitive Teichmüller curves, the arabesque series $A_D \subset \mathcal{M}_4$. The terminology for G_D and A_D is inspired by their polygonal models shown in Figure 8.1.

Curves and surfaces. Let $\mathcal{M}_{g,n}$ denote the moduli space of compact Riemann surfaces A of genus g with n unordered marked points $P \subset A$. We will begin by constructing the flex locus

$$F \subset \mathcal{M}_{1,3}$$

the gothic locus

$$\Omega G \subset \Omega \mathcal{M}_4(2^3),$$

and the gothic curves $G_D \subset \mathcal{M}_4$. We will then sketch the proof of the following results.

Theorem 8.1. The flex locus F is a primitive, totally geodesic surface in $\mathcal{M}_{1,3}$.

The fact that F is totally geodesic will follow from:

Theorem 8.2. The gothic locus ΩG is $\mathrm{SL}_2(\mathbb{R})$ -invariant.

Theorem 8.3. Each component of $G_D \subset \mathcal{M}_4$ is a primitive Teichmüller curve.

Explicit examples of gothic curves coming from billiards in quadrilaterals will be given in §9. Since these curves are generated by forms in $\Omega \mathcal{M}_4(2^3)$, rather than $\Omega \mathcal{M}_4(6)$, we obtain:

Table 8.1. Euler characteristics of gothic curves.

D	N_D	$\chi(G_D^{\epsilon})$	D	N_D	$\chi(G_D^{\epsilon})$
12	1	-1/2	60	1	-16/3
24	1	-7/6	72	1	-26/3
28	2	-5/3	73	4	-29/3
33	2	-8/3	76	2	-49/6
40	2	-19/6	84	1	-13
48	1	-5	88	2	-59/6
52	2	-13/2	96	1	-16
57	2	-6	97	4	-44/3

Corollary 8.4. There exist infinitely many primitive Teichmüller curves in genus 4 that are not accounted for by the Weierstrass series $W_D \subset \mathcal{M}_4$.

The gothic locus $\Omega G \subset \Omega \mathcal{M}_4$ is an analogue, in genus four, of the stratum $\Omega \mathcal{M}_2(2)$ in genus two. Each of these 4-dimensional varieties provides a *substrate* on which one can impose the additional constraint of real multiplication, to obtain the Teichmüller curves G_D and W_D respectively.

Topology. The following result describes when G_D is nonempty, gives a lower bound N_D on its number of components, and computes its Euler characteristic.

Theorem 8.5 (Möller–Torres-Teigell). The gothic curve G_D is nonempty iff D is a square mod 24. It falls into $N_D = 1, 2$ or 4 subcurves G_D^{ϵ} of equal Euler characteristic, and one can express $\chi(G_D^{\epsilon})$ in terms of $\chi(\mathfrak{X}_D)$ and an elementary sum.

Here ϵ runs from 1 to N_D , which is the number of ideals of norm 6 in \mathcal{O}_D . Explicitly, we have $N_D=1,2$ or 4 for $D \mod 24 \in \{0,12\},\{4,9,16\}$ or $\{1\}$, respectively; otherwise $N_D=0$. See Table 8.1 for a table of invariants of the gothic curves with $D \leq 100$. It is unknown at present if G_D^ϵ is irreducible.

Plane cubics. We now turn to the construction of the flex locus $F \subset \mathcal{M}_{1,3}$.

First we recall some classical constructions in projective geometry. Every Riemann surface of genus 1 can be realized, in an essentially unique way, as a smooth cubic curve $A \subset \mathbb{P}^2$. Algebraically, A = Z(f) is the zero locus of a homogeneous cubic polynomial $f: \mathbb{C}^3 \to \mathbb{C}$.

Given a point $S = [s_0, s_1, s_2] \in \mathbb{P}^2$, the *polar conic* of A with respect to S is defined by

$$\operatorname{Pol}(A, S) = Z\left(\sum s_i \frac{df}{dx_i}\right).$$

Projection from S to a line defines a rational map

$$\pi_S:A\to\mathbb{P}^1,$$

and

$$A \cap \text{Pol}(A, S) = \{\text{critical points of } \pi_S\}.$$

Provided $S \notin A$, π_S has degree 3 and 6 critical points.

Let $T_xA \subset \mathbb{P}^2$ denote the tangent line to A at x. The polar conic picks out the six points $x \in A$ such T_xA passes through S. For each such x, there is a unique cocritical point x' such that

$$T_x A \cap A = \{x, x'\}.$$

Equivalently, $\{x, x'\}$ is a fiber of π_S . The six cocritical points of π_S lie on the satellite conic $\operatorname{Sat}(A, S)$.

The Hessian. The cubic curve A canonically determines a second cubic, its $Hessian\ HA = Z(\det D^2 f)$. The intersection $A \cap HA$ coincides with the 9 flexes of A. Classically, one picks a flex to serve as the origin for the group law on A; then the set of all flexes corresponds to the subgroup A[3] of points of order 3.

Dusk and dawn. The Hessian can also be related to the polars of A: we have

$$HA = \{ S \in \mathbb{P}^2 : \text{ the polar conic } Pol(A, S) \text{ is singular} \}.$$

When $S \in HA$, both the polar conic and the satellite conic degenerate to a pair of lines:

$$\operatorname{Pol}(A, S) = L_1 \cup L_2$$
 and $\operatorname{Sat}(A, S) = L'_1 \cup L'_2$.

To better visualize this solar configuration, imagine that the cubic A represents a (strangely shaped) planet, illuminated by rays from the sun S. The sun lies on the horizon, as seen from $x \in A$, exactly when the tangent line to A at x passes through S; equivalently, when $x \in \text{Pol}(A, S)$. Thus it is twilight at six points of A.

In the solar configuration, we can naturally divide these six points into two groups of three, $L_1 \cap A$ and $L_2 \cap A$, which we call dawn and dusk. The 3 rays of dawn also meet A at three other points, namely $L'_1 \cap A$, which we call the codawn points; see Figure 8.2.

The flex locus. The flex locus $F \subset \mathcal{M}_{1,3}$ records the set of all possible configurations of codawn points $P \subset A$. More precisely,

$$F = \left\{ (A, P) \in \mathcal{M}_{1,3} : \begin{array}{c} P = A \cap L \text{ for some point } S \in HA \\ \text{and line } L \subset \text{Sat}(A, S) \end{array} \right\}.$$

The terminology comes from the fact that $\det D^2 f = 0$ at S. Since there are two choices for L, the fiber of F over $A \in \mathcal{M}_1$ is actually parameterized by a double cover $CA \to HA$, classically called the Cayleyan of A. Thus F is the image of an elliptic surface; however the map $CA \to F$ is not injective, and F itself is birational to \mathbb{P}^2 .

The gothic locus. We now turn to the construction of the space ΩG from F.

Recall that any Riemann surface $X \in \mathcal{M}_g$ which is not hyperelliptic admits a canonical embedding

$$X \hookrightarrow \mathbb{P}\Omega(X)^* \cong \mathbb{P}^{g-1}$$

of degree 2g-2. This embedding is characterized by the property that its hyperplane sections $H\cap X$ coincide with the zero sets of holomorphic 1-forms $0\neq\omega\in\Omega(X)$. In the case g=4, there exist quadric and cubic hypersurfaces Q and C such that

$$X = Q \cap C \subset \mathbb{P}^3$$
.

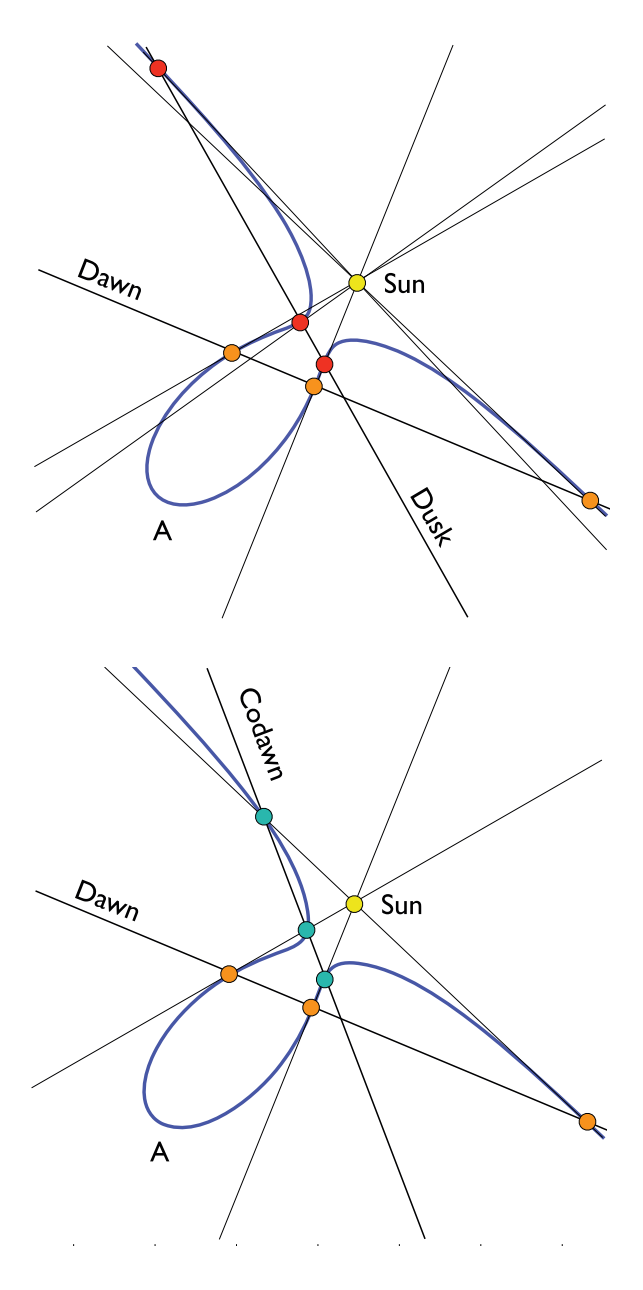


FIGURE 8.2. The solar configuration.

To facilitate the passage between two and three dimensions, choose an involution J on \mathbb{P}^3 such that

$$\operatorname{Fix}(J) = \mathbb{P}^2 \cup \mathbb{P}^0.$$

Now consider a solar configuration as above: a cubic curve $A \subset \mathbb{P}^2$, a point $S \in HA - A$, and a codawn line D with $P = D \cap A$. Choose a second line L

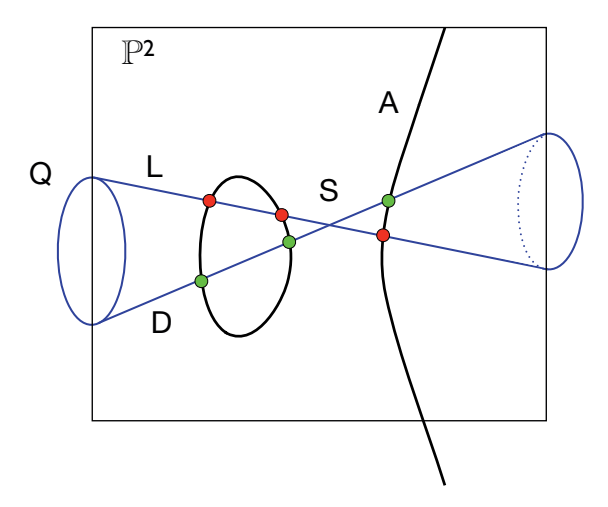


FIGURE 8.3. The canonical curve X of genus 4 is the intersection of Q and the cone over A.

through S, transverse to A. We can then find quadric and cubic surfaces Q, C in \mathbb{P}^3 , such that:

- J(Q) = Q and J(C) = C;
- $Q \cap \mathbb{P}^2 = D \cup L$; and
- C is the cone over A with vertex \mathbb{P}^0 .

In this way a solar configuration, together with an additional line L through S, naturally determines a curve of genus 4, namely

$$X = Q \cap C$$
.

See Figure 8.3.

There is a unique hyperplane H tangent to Q along L, and hence a 1-form ω on X such that $(\omega) = H \cap L$. Because of the tangency, the zeros of ω have multiplicity two.

The gothic locus $\Omega G \subset \Omega \mathcal{M}_4(2^3)$ consists of all forms (X, ω) arising as above. Since X is determined by the solar configuration plus a line through S, and ω is unique up to a scale factor, we have $\dim \Omega G = \dim F + 2 = 4$. We also have a natural degree two map

$$p: X \to A$$
,

obtained by projection from \mathbb{P}^0 ; and a natural map $\Omega G \to F$, forgetting ω and the extra line L.

The Abelian surface carrying ω . We need to introduce one more key player before we can define the gothic curves G_D .

Note that the composition $\pi_S \circ p : X \to \mathbb{P}^1$ has degree 6. The target \mathbb{P}^1 of π_S can be naturally identified with the space of lines through S.

Let $B \to \mathbb{P}^1$ be the elliptic curve obtained as a 2-fold covering of \mathbb{P}^1 branched over the three lines of dusk and the extra line L determining X. One can then

verify that there is a unique degree three map $q: X \to B$ making the diagram

commute. One also check that

(8.2)
$$p_*(\omega) = q_*(\omega) = 0.$$

By pulling back line bundles from A and B to X, we obtain an exact sequence

(8.3)
$$\operatorname{Jac}(A) \oplus \operatorname{Jac}(B) \to \operatorname{Jac}(X) \to C \to 0,$$

with dim $C = \dim \operatorname{Jac}(X) - 2 = 4$. We refer to C as the *hidden Abelian surface* attached to (X, ω) . Identifying $\Omega(C)$ with a subspace of $\Omega(X)$, equation (8.2) implies:

We have $\omega \in \Omega(C)$ for all forms (X, ω) in the gothic locus.

The gothic curves. Let $\Omega G_D \subset \Omega G$ denote the 2-dimensional locus where ω is an eigenform for real multiplication by \mathcal{O}_D on C. The gothic curve G_D is defined, finally, as the projection of ΩG_D to \mathcal{M}_4 .

Sketch of the proofs. To conclude, we sketch the proofs of Theorems 8.1, 8.2 and 8.3. The main point is:

1. ΩG is $\mathrm{SL}_2(\mathbb{R})$ -invariant. Note that the gothic locus is 4-dimensional, and that the gothic forms satisfy

$$[\omega] \in H^1(C) \subset H^1(X, Z(\omega)).$$

Since dim $H^1(C) = 4$ as well, ΩG is locally defined by the condition above, which is given by real linear equations in period coordinates. Invariance under $\mathrm{SL}_2(\mathbb{R})$ follows.

- 2. F is totally geodesic. The $SL_2(\mathbb{R})$ orbits in ΩG project to complex geodesics in F. Since dim $\Omega G = 4$ and dim F = 2, there is a pencil of geodesics through every point of F, and hence F is totally geodesic.
- 3. G_D is a finite union of Teichmüller curves. We have seen that ΩG is $\mathrm{SL}_2(\mathbb{R})$ -invariant, and by invariance of quadratic real multiplication, so is ΩG_D . Thus its projection to \mathcal{M}_4 is a totally geodesic curve G_D .

9. Quadrilaterals

In this section we will see that the gothic curves, and the flex locus, belong to a suite of examples naturally associated to six types of quadrilaterals.

This suite yields:

- (1) six examples of $SL_2(\mathbb{R})$ -invariant 4-folds in $\Omega \mathcal{M}_q$, for various g;
- (2) three examples of primitive, totally geodesic surfaces in $\mathcal{M}_{g,n}$, for various (g,n);
- (3) two distinct series of Teichmüller curves in \mathcal{M}_4 ; and
- (4) two families of quadrilateral billiard tables with optimal dynamical properties.

In particular, the quadrilaterals of type (1, 1, 2, 8) will yield our last family of Teichmüller curves, the *arabesque series* $A_D \subset \mathcal{M}_4$. We follow the development in [EMMW].

Cyclic forms. It is convenient to describe the type of a quadrilateral by a quadruple of integers a. We require that the integers $a = (a_1, a_2, a_3, a_4)$ are positive and relatively prime, that

$$2m = a_1 + a_2 + a_3 + a_4$$

is even, and that $a_i \neq m$ for all i.

Each quadruple a determines a family of cyclic forms $\Omega Z_a \subset \Omega \mathcal{M}_g$. Such a form can be specified by four distinct branch points (b_i) in \mathbb{C} ; it is then given by $\omega = dx/y$ on the curve X defined by

(9.1)
$$y^m = \prod_{i=1}^{4} (x - b_i)^{m - a_i}.$$

The cyclic forms contain the unfoldings of every quadrilateral with internal angles $\theta_i = \pi(a_i/m)$, in any order; the quadrilateral's vertices correspond to the branch points $b_i \in \mathbb{R}$.

Let $\zeta_m = \exp(2\pi i/m)$. Note that $r(x,y) = (x,\zeta_m^{-1}y)$ gives an automorphism of X of order m, satisfying $r^*(\omega) = \zeta_m \omega$. Thus the symmetric correspondence

$$Y = \{(p,q) : q = r^{\pm 1}(p)\} \subset X \times X$$

determines a self-adjoint endomorphism T of Jac(X), satisfying

(9.2)
$$T^*(\omega) = (\zeta_m + \zeta_m^{-1})\omega.$$

Action of $SL_2(\mathbb{R})$. The smallest closed invariant set containing the cyclic forms of type a is its saturation

$$\Omega G_a = \overline{\mathrm{SL}_2(\mathbb{R}) \cdot \Omega Z_a} \subset \Omega \mathcal{M}_g.$$

Our first result describes this space.

Theorem 9.1. For each of the six values of a listed in Table 9.1, the saturation of the cyclic forms gives a primitive, irreducible, 4-dimensional invariant subvariety $\Omega G_a \subset \Omega \mathcal{M}_q$.

The remarkable feature of these six cases is that, while the action of $SL_2(\mathbb{R})$ destroys the cyclic symmetry of forms in ΩZ_a , it merely deforms the correspondence $Y \subset X \times X$ as an algebraic cycle. The relation (9.2) persists under deformation, and the original cyclic symmetries of X are replaced by an action of the dihedral group

$$D_{2m} = \langle r, f : r^m = f^2 = (rf)^2 = id \rangle$$

on Y, satisfying $X = Y/\langle f \rangle$. The main step in the proof of Theorem 9.1 is to show the resulting variety of *dihedral forms* is 4-dimensional; its closure must then coincide with ΩG_a . The requirement that dim $\Omega G_a = 4$ singles out the six values of a in Table 9.1.

,			I
(a_1, a_2, a_3, a_4)	m	Stratum of ΩG_a	$F_a \subset \mathcal{M}_{g,n}$
(1, 1, 1, 7)	5	$\Omega \mathcal{M}_4(6)$	
(1, 1, 1, 9)	6	$\Omega \mathcal{M}_4(2^3)$	$\mathcal{M}_{1,3}$
(1, 1, 2, 8)	6	$\Omega \mathcal{M}_4(3^2)$	
(1, 1, 2, 12)	8	$\Omega \mathcal{M}_5(2^4)$	$\mathcal{M}_{1,4}$
(1, 2, 2, 11)	8	$\Omega \mathcal{M}_6(10)$	
(1, 2, 2, 15)	10	$\Omega \mathcal{M}_6(2^5)$	$\mathcal{M}_{2,1}$

Table 9.1. Six types of quadrilaterals and their associated varieties.

Teichmüller curves. By equation (9.2), $[\omega]$ is an eigenvector for $T|H^1(X)$ with eigenvalue $\lambda_m = \zeta_m + \zeta_m^{-1} = 2\cos(2\pi/m)$. Let $H^1(C) = \text{Ker}(T - \lambda_m I)$ denote the full eigenspace. Provided λ_m is rational, this subspace is of geometric origin: namely, it comes from a map to an Abelian surface,

$$\operatorname{Jac}(X) \to C$$
.

Let $\Omega G_{a,D}$ denote the locus where ω is an eigenform for real multiplication by \mathcal{O}_D on C, and let $G_{a,D}$ denote its projection to \mathcal{M}_q . As in §8, we then obtain:

Theorem 9.2. For a = (1, 1, 1, 9) or (1, 1, 2, 8), locus $G_{a,D} \subset \mathcal{M}_4$ is a finite union of primitive Teichmüller curves for each discriminant D.

These curves come from the two entries in Table 9.1 where m=6; for the other entries, $\cos(2\pi/m)$ is irrational.

The arabesque series A_D . The gothic locus ΩG coincides with ΩG_a for a=(1,1,1,9), and thus $G_D=G_a,D$ as well. But the curves in the arabesque series, defined by

$$A_D = G_{a,D}$$
 with $a = (1, 1, 2, 8)$,

are new; they constitute the last known series of primitive Teichmüller curves. At present, neither G_D nor A_D is as well–understood as the Weierstrass curves.

Determine the number of components of the curves A_D and G_D . Are any two components of the same curve homeomorphic? What are their topological invariants?

Billiards. Using the relation with cyclic forms, one can readily give explicit generators for gothic and arabesque Teichmüller curves; see Figure 9.1.

Theorem 9.3. Billiards in the quadrilateral $Q_{1119}(1, \sqrt{3}y)$ has optimal dynamics, and the associated cyclic 1-form generates a gothic Teichmüller curve in \mathcal{M}_4 , provided y > 0 is irrational and

$$y^2 + (3c+1)y + c = 0$$

for some $c \in \mathbb{Q}$. The quadrilateral $Q_{1128}(1,y)$ similarly generates an arabesque curve, provided $y^2 + (2c+1)y + c = 0$.

Problem 9.4. The cases c = -1/4 and c = -1 are shown at the left and right, respectively, in Figure 9.1. An unfolding of the polygon on the right appears Figure 8.1.

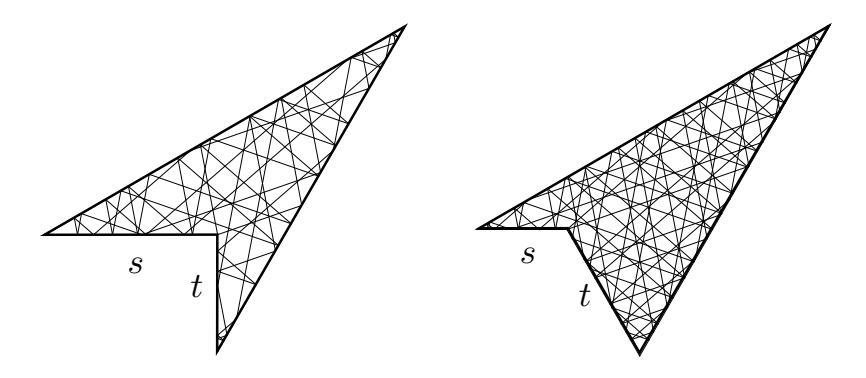


FIGURE 9.1. Closed billiard paths in $Q_{1119}(s,t)$ and $Q_{1128}(s,t)$.

Teichmüller surfaces. Finally we describe generalizations of the flex surface. We will see that the perspective of quadrilaterals leads to a unified construction of three remarkable and unexpected Teichmüller surfaces in moduli space.

First suppose that m is even. We then have a natural map π from $\Omega G_a \subset \Omega \mathcal{M}_g$ to a variety F_a in a moduli of lower dimension. The point $(A, P) = \pi(X, \omega)$ is constructed by first forming the quadratic differential $(A, q) = (X, \omega)/\langle r^{m/2} \rangle$, and then marking the poles P of q.

The fibers of π are 2-dimensional exactly when m/2 divides one of (a_1, a_2, a_3, a_4) . To see why this might be the case, observe that for $(X, \omega) \in \Omega Z_a$ the curve A is defined by equation (9.1) with y^m replaced by $y^{m/2}$. If m/2 divides a_i , then A is only branched over the three points b_j , $j \neq i$. Since a configuration of three points on \mathbb{P}^1 has no moduli, π sends the entire 2-dimensional locus ΩZ_a to a single point $(A, P) \in F_a$.

When the fibers of π are 2-dimensional, the $\mathrm{SL}_2(\mathbb{R})$ -invariance of ΩG_a shows F_a is a totally geodesic surface, just as in the proof of Theorem 8.1. Summarizing, the final result is:

Theorem 9.5. The locus $F_a \subset \mathcal{M}_{g,n}$ is a primitive, irreducible, totally geodesic surface for the three cases indicated in Table 9.1.

The case a = (1, 1, 1, 9) gives the flex surface in $\mathcal{M}_{1,3}$; the other two examples reside in $\mathcal{M}_{1,4}$ and $\mathcal{M}_{2,1}$. In each case, the cyclic locus ΩZ_a projects to the unique point in $\mathcal{M}_{g,n}$ with a cyclic symmetry of order m/2 = 3, 4 or 5.

Local geodesic flatness. Here is an indication of why a primitive, totally geodesic variety $F \subset \mathcal{M}_{g,n}$ of dimension greater than one is so unusual—even more unusual than a Teichmüller curve.

For each $(A, P) \in F$, let

$$Q(A,P) \cong T_{(A,P)}^* \mathcal{M}_{g,n}$$

denote the space of holomorphic quadratic differentials on A-P with at worst simple poles at P. This finite–dimensional vector space is endowed with a natural L^1 -norm, given by $||q|| = \int_A |q|$.

Let $F \subset \mathcal{M}_{g,n}$ be a totally geodesic variety of dimension d. Given $(A, P) \in F$, the cotangent vectors that annihilate $T_{(A,P)}F$ give a natural subspace $N \subset Q(A,P)$

of codimension d. Let

$$QF(A,P) = \left\{ q \in Q(A,P) : \int_A \frac{n\overline{q}}{|q|} = 0 \ \forall n \in N \right\}.$$

The quadratic differentials in QF(A, P) are those which generate geodesics in F through (A, P). By convention, we include q = 0 in QF(A, P).

Despite its nonlinear definition, the cone QF(A, P) is a linear subspace of Q(A, P) in all known examples, including those in Theorem 9.5.

The linearity of QF(A,P) is automatic when $\dim F=1$, but for d>1 it reflects an unusual property of N inside the normed vector space Q(A,P). Indeed, QF(A,P) records the supporting hyperplanes for the *unit ball* in $Q(A,P)^*$ along its intersection with N^{\perp} . This ball is a complicated convex body, and for most N, the locus QF(A,P) defined above is not even a real–analytic set.

It is true that isometric symmetries of Q(A, P) may force QF(A, P) to be linear. But these symmetries are typically ruled out by the assumption that F is primitive. It is thus remarkable that F exists at all. As a complement to the problem of classifying Teichmüller curves, we conclude with:

Problem 9.6. Construct and classify all primitive totally geodesic varieties $F \subset \mathcal{M}_{q,n}$ with $\dim(F) > 1$.

It seems likely we are still in the age of discovery.

10. Notes and references

§1. Introduction. For an algebraic perspective on \mathcal{M}_g , and the realization of its Deligne–Mumford compactification as a projective variety, see [ACG].

The dilatation $K(A) \geq 1$ of a real-linear map $A : \mathbb{C} \to \mathbb{C}$ is given by the ratio M/m between the major and minor axes of the image of a circle under A. The dilatation of an orientation-preserving diffeomorphism $f : X \to Y$ between Riemann surfaces is given by $\sup_x K(Df_x)$, and the Teichmüller metric on \mathcal{M}_g is given by

$$d(X,Y) = \frac{1}{2} \inf_{f} \log K(f).$$

This metric also comes from the natural norm $||q|| = \int_X |q|$ on the cotangent space $T_X^* \mathcal{M}_g$, which can be identified with the space of holomorphic quadratic differentials $q = q(z) dz^2$ on X. For background in Teichmüller theory, see, e.g. [Ga], [Nag] and [Hub].

Figure 1.2 shows the generalized polygon $T_{60,40}$ discussed at the end of §7.

The five known horizontal series of Teichmüller curves all involve real multiplication by an order \mathcal{O}_D in a real quadratic field. According to [EFW, Thm. 1.5], any horizontal series must have this feature. The proof that these curves are totally geodesic relies on an argument in §4, showing that quadratic real multiplication is $\mathrm{SL}_2(\mathbb{R})$ -invariant.

§2. Moduli spaces and Teichmüller curves. For a proof of Theorem 2.2 with $P \subset \mathbb{C}$ embedded and connected, see [Vi, Cor. 3.34].

Every complex geodesic $f: \mathbb{H} \to \mathbb{C}$ is generated by a quadratic differential (X, q).

We have concentrated on the case where $q=\omega^2$ arises from a 1-form, for several reasons:

- (1) Any quadratic differential (X, q) becomes the square of a 1-form after passing to a 2-fold branched covering of X.
- (2) Therefore, every Teichmüller curve generated by a quadratic differential is a close relative of one generated by a primitive 1-form.
- (3) Finally, a holomorphic 1-form represents a cohomology class $[\omega] \in H^1(X)$ and a differential on the Jacobian of X, providing a bridge to Hodge theory.

For the stated properties of the trace field K, see [GJ, Thm. 5.5], [KS, Thm. 28], [Ho2, Thm. 10.2] and [HL, Thm. 1.1].

The mild twisting of the action of $\mathrm{SL}(X,\omega)$, mentioned after equation (2.6), arises as follows. Let $K=\mathrm{SO}_2(\mathbb{R})\subset G=\mathrm{SL}_2(\mathbb{R})$. The isometric action of G on \mathbb{H} gives an isomorphism $G/K\cong \mathbb{H}$ sending A to A(i). The linear action of G on $\mathbb{R}^2\cong \mathbb{C}$ gives a second isomorphism, $K\backslash G\cong \mathbb{H}$, sending A to A(i)/A(1). One can then readily check that the bijection $G/K\cong K\backslash G$, given by $A\mapsto A^{-1}$, induces the map $t\mapsto -\overline{t}$ from \mathbb{H} to itself. One must conjugate by this map to convert the linear action of $\mathrm{SL}(X,\omega)$ into an action by Möbius transformations on \mathbb{H} . See [Mc1, Prop. 3.2].

As a complement to Proposition 2.3, we remark that the condition $D\phi = \begin{pmatrix} 1 & 1/m \\ 0 & 1 \end{pmatrix}$, m > 0, does *not* imply that m divides $\text{mod}(C_i)$ for all horizontal cylinders C_i . For example, ϕ may effect a fractional Dehn twist on some C_i , or even permute these cylinders.

Smillie has shown that (X, ω) generates a Teichmüller curve if and only if $SL_2(\mathbb{R})$ · (X, ω) is closed in $\Omega \mathcal{M}_g$ [V2, §6].

§3. Billiards. The fundamental result on the Veech dichotomy, Theorem 3.2, appears in [V1, Prop. 2.11]. The proof using [Mas2] presented here (see also [HS2, §1.4]) bridges a gap in the original argument, noted in [Mc1, §2].

The polygon in Figure 3.2 is a square S with a generic rectangle R attached. The trajectory shown, with starting slope 1, would be periodic if R were absent.

Rational polygons have special properties. For example, it is unknown if every triangle has a periodic billiard trajectory; cf. [Sch1]. On the other hand, if P has angles in $\pi\mathbb{Q}$, then it has a dense set of periodic slopes and a full measure set of uniformly distributed directions [Mas1], [KMS]. (These two papers are among the first to use Teichmüller theory to address the dynamics of billiards.)

The algebraic description of the Teichmüller curves generated by regular polygons originates in [Loch]; see also [Mc4, §5] and [EMMW, Appendix A].

For more on relations between the golden table and the regular pentagon, see $[Mc1, \S 9 \text{ and Fig. 4}]$ and [DL]. Periodic slopes on general Teichmüller curves are studied in [Mc10].

Question 3.8 is implicit in [HMTY], and stated explicitly in [Bo] as Conjecture 1.4; see these works for more on periodic slopes in the regular heptagon. Winsor has shown that $\Delta(2,7,\infty)$ has more than two orbits in $\mathbb{Q}(\cos(\pi/7)) \cup \{\infty\}$, contrary to a conjecture in [HMTY, §4.1]; e.g. x=671 lies outside the previously known orbits. Experimentally, x=2 is not fixed by any hyperbolic or parabolic element in $\Delta(2,p,\infty)$ when $p \geq 11$ is odd.

The discovery and classification of the lattice triangles appearing in Theorem 3.9 is contained in the work of several authors. Series A, along with the series of regular polygons, is discussed in [V1]. For series B, see [Vo2, Thm. 4.4] and [Wa]. Two of the three sporadic triangles in C also appear in [Vo2]; for the (2,3,4) example, see [KS]. Example D is from [Ho1]. The proof that this list of lattice triangles is complete, apart from the obtuse, scalene case, is given in [KS], [Pu1] and [Pu2].

For recent work on Question 3.11, see [LNZ].

The lattice polygons of genus two are classified in [Mc4].

Despite the Veech dichotomy, long, periodic trajectories in a lattice polygon can be unevenly distributed; see [DL], [Mc9].

§4. Genus 2. Every form (X, ω) of genus two can be presented, in infinitely many ways, as the connect sum $(E_1, \omega_1) \# (E_2, \omega_2)$ of a pair of forms of genus one. This perspective plays a central role in the proof of Theorems 4.1, 4.2 and 4.5, in [Mc2], [Mc1] and [Mc4], respectively; it also leads to an explicit classification of the orbit closures and the ergodic invariant measures for $SL_2(\mathbb{R})$ acting on $\Omega \mathcal{M}_2$ [Mc5].

Veech groups for several W_D are shown in [Mc1, Fig. 5] and [Mc4, Fig. 2]. Theorem 4.3 is given in detail in [Mc2, Cor. 1.3]. Theorem 4.5 leads to many simple examples of 1-forms such that $SL(X,\omega)$ is an infinitely generated group [Mc4, Thm. 1.3]. For related work, see [HS1].

Theorem 4.7 and formula (4.2), appear in [Ba, Thms. 1.1 and 2.12]. In [MZ, Thm. 9.1], Möller and Zagier show $W_D \subset \mathfrak{X}_D$ is the zero locus of an explicit Hilbert modular form of weight (3,9), namely

(10.1)
$$f_D(z) = \prod_{(m,m') \text{ odd}} D_2 \theta_{(m,m')}(z_1, z_2).$$

The Euler characteristic of W_D is directly related to the weights of this form; in brief, dz_1 and dz_2 give line bundles L_1, L_2 over \mathfrak{X}_D , and

$$\chi(W_D) = -\langle c_1(L_1), W_D \rangle = -(9/2)\langle c_1(L_1), c_1(L_2) \rangle = -(9/2)\chi(\mathfrak{X}_D),$$

since $2[W_D] = 3c_1(L_1) + 9c_1(L_2)$ up to boundary terms.

For Theorem 4.8 on elliptic points, and the remarks on $g(W_D)$ that follow, see [Mu1]. Algebraic models for W_D with D=13 and 17 are given in [BM1], and for all fundamental discriminants D<100 in [KM2].

Theorem 4.6 can be deduced from the fact that W_D^0 and W_D^1 are Galois conjugate [BM1, Thm. A]. It also follows directly from the calculations in [Mc2], [Ba] and [Mu1], which show the topological invariants of W_D^ϵ do not depend on ϵ .

Theorem 4.12 is contained in [Mo1] and [Mo2].

The classification of nonprimitive Teichmüller curves in \mathcal{M}_2 is still an open problem; see [Du] for the conjectural answer and recent progress. Integral polynomials defining W_{d^2} , given in [Mu2], behave well mod p and suggest an arithmetic theory of Teichmüller curves remains to be developed.

§5. Genus 3 and 4. The definition of W_D using Prym varieties, and the proof of Theorem 5.1, appear in [Mc3]. Examples of Veech groups for Weierstrass curves in genus g = 3 and 4 are shown in [Mc3, Fig. 2].

The classification of Weierstrass curves given in Theorem 5.3 appears in [LN1] and [LN2].

The finiteness Theorem 5.5 appears to be stated here for first time. It follows from two known results. First, by [EFW, Thm. 1.5], all but finitely many primitive Teichmüller curves in \mathcal{M}_g are obtained by imposing quadratic real multiplication on a 4-dimensional, rank 2, $\mathrm{SL}_2(\mathbb{R})$ -invariant subvariety $M \subset \Omega \mathcal{M}_g$, defined over \mathbb{Q} in period coordinates. Second, the classification of such M in genus three is now known; see [AN, Thm. 1.1] and the references therein. There are three examples; but two of them are contained in the hyperelliptic locus, and consist of forms pulled back from genus two, so the associated Teichmüller curves are not primitive. The one remaining possibility for M gives rise to the Weierstrass curves $W_D \subset \mathcal{M}_3$.

For progress toward making Theorem 5.5 more effective, see [BaM, Thm. 1.6] and [LM]. A related result, [EFW, Cor. 1.6], states that for each g there are only finitely many Teichmüller curves in \mathcal{M}_g with trace field of degree 3 or more. For general finiteness results in hyperelliptic strata, see [Ap].

The formulas for $\chi(W_D)$ in Theorem 5.7 appear in [Mo5, Thm. 0.2]; their calculation uses theta functions and Hilbert modular forms (for the case g=2, see equation (10.1)).

See [Za] for Theorem 5.6, and [TZ1] and [TZ2] for Theorem 5.8.

§6. Multicurves and Coxeter diagrams. Thurston's multicurve construction appears in [Th]. Our presentation follows [Mc3, §4], which also proves Theorem 6.4. The set of all multicurve systems encoding a given Teichmüller curve is described in [Mc9, §10].

Coxeter groups and their diagrams appear in many fields of mathematics, ranging from Lie groups and sphere packings to singularity theory; useful references include [Bou] and [Hum]. Theorem 6.2, with different terminology, is contained in [Lei, Thm. 7.1]. The formulation and short proof we present here emphasize the direct connection with Coxeter groups. Theorem 6.3, relating the sporadic lattice triangles to the E_n diagrams, was proposed in [Mc11] and proved in [Lei, §7.5].

We remark that the Coxeter element $\rho_A \rho_B$ for $\Gamma(A, B)$, and the multitwists τ_A and τ_B , both act on $\mathbb{R}^A \oplus \mathbb{R}^B$ and are related by

$$-\rho_A \rho_B = -\begin{pmatrix} -I & M \\ 0 & I \end{pmatrix} \begin{pmatrix} I & 0 \\ M^t & -I \end{pmatrix} = \begin{pmatrix} I & M \\ 0 & I \end{pmatrix} \begin{pmatrix} I & 0 \\ -M^t & I \end{pmatrix} = \tau_A \tau_B.$$

This explains why Coxeter numbers (which give the order of $\rho_A \rho_B$) appear in Table 6.1 (up to a factor of two).

We note that the E_6 triangle unfolds to a Riemann surface $X \in \mathcal{M}_3$ which lies on the unique Shimura–Teichmüller curve $V \subset \mathcal{M}_3$. Indeed X, initially defined by $y^{12} = x^3(x-1)^4$, is isomorphic to $v^3 = u^4 - 1$ (by the change of variables $(x,y) = (u^4,uv)$), and the latter curve represents a point on V by [Mo4, Thm. 5.1]. The E_7 Teichmüller curve is studied in [CK].

§7. Higher genus. The original construction of V_{pq} appears in [BM2]. Its reformulation in terms of semiregular polygons was discovered independently by Mukamel and Hooper. We follow [Ho2] for much of this section; see also [Wr1].

Both $T_m(x)$ and $\widetilde{T}_m(x)$ are separable polynomials of degree m with integral coefficients. In terms of the Chebyshev polynomials $U_m(x)$ of the second kind, we have

$$\widetilde{T}_m(x) = U_{2m}(\sqrt{(1+x)/2}) = U_m(x) - U_{m-1}(x).$$

The roots of $T_m(x)$ occur when $x = \cos \theta$ and $\cos m\theta = 0$; those of $\widetilde{T}_m(x)$ occur when $\cos(2m+1)\theta = 1$, but $\cos \theta \neq 1$.

For Theorem 7.3, see [BM2, Thm. 6.14] and [Ho2, Thm. 4.9]. We have streamlined the formulas by using the intermediate variable z and Chebyshev polynomials, to better display the integrality of the coefficients.

Theorem 7.6 is based on [Ho2, Thm. 4.1].

Note that T_{pq} gives an explicit, embedded lattice polygon for all $p \leq 5$. As can be seen in Figure 7.4, T_{pq} is also embedded for 8 other values of (p,q), and its interior is embedded for 2 more values. This list of lattice polygons broadens that appearing in [BM2, §8].

The rectilinear cousin $(X, \omega)_{p,2}$ of the *p*-sided regular polygon is discussed in detail in [Mc6, §13], from the perspective of braid groups and the A_{p-1} diagram.

§8. Gothic curves and the flex locus. Theorems 8.1, 8.2, 8.3, and Corollary 8.4 are taken from [MMW]. For Theorem 8.5, see [MT, Thm. 11.1]; Table 8.1 is an excerpt of Table 1 in the same reference. We note that G_D can also be defined by imposing real multiplication on the dual Abelian surface $\hat{C} \subset \operatorname{Jac}(X)$; this equivalent perspective is adopted in [MT].

For the classical theory of plane cubics, their polars, the Hessian and related topics, see [Sal].

§9. Quadrilaterals. All theorems stated in this section appear in [EMMW, §1]. The totally geodesic surface $F_a \subset \mathcal{M}_{2,1}$, a = (1, 2, 2, 15), is also studied in [KM1]. Regarding Problem 9.6, Wright has shown [Wr4] that for each g, there are only finitely many totally geodesic subvarieties $F \subset \mathcal{M}_g$ with $\dim(F) > 1$. For more on QF(A, P) in the case of the flex locus, see [MMW, §4].

APPENDIX A. TRIANGLE GROUPS

Let p, q be positive integers with 1/p + 1/q < 1. We define the (p, q, ∞) triangle group by

$$\Delta(p, q, \infty) = \langle S, T \rangle \subset \mathrm{SL}_2(\mathbb{R}),$$

where

$$S = \begin{pmatrix} \cos(\pi/p) & \sin(\pi/p) \\ -\sin(\pi/p) & \cos(\pi/p) \end{pmatrix} \quad \text{and} \quad T = \begin{pmatrix} 1 & \tau \\ 0 & 1 \end{pmatrix},$$

and τ is chosen so that $\text{Tr}(ST) = -2\cos(\pi/q)$. Its invariant trace field is given by:

$$K_{pq} = \mathbb{Q}(\operatorname{Tr}(g^2) : g \in \Delta(p, q, \infty))$$

= $\mathbb{Q}(\cos(2\pi/p), \cos(2\pi/q), \cos(\pi/p)\cos(\pi/q)).$

This field is a commensurability invariant.

The quotient space $X = \mathbb{H}/\Delta(p,q,\infty)$ is an orbifold isometric to the double of the unique hyperbolic triangle with internal angles π/p , π/q and $\pi/\infty = 0$. We also allow $q = \infty$, in which case Tr(ST) = -2 and X has two cusps.

The groups $\Delta(p, q, \infty)$ and $\Delta(q, p, \infty)$ are conjugate in $\mathrm{SL}_2(\mathbb{R})$. When p and q are both even, we have a natural subgroup of index two

$$\widetilde{\Delta}(p/2, q/2, \infty, \infty) \subset \Delta(p, q, \infty),$$

corresponding to the orbifold covering space $Y \to X$ branched over the points of X of orders p and q. As indicated by the notation, Y has two cusps. (Note that $\widetilde{\Delta}(p, 1, \infty, \infty)$ is isomorphic to $\Delta(p, \infty, \infty)$.)

When p is odd, we let

$$\Delta^{-}(p, \infty, \infty) = \langle -S, T \rangle.$$

This group has index two in $\Delta(p, \infty, \infty)$, and it does *not* contain -I. All the other groups above do contain -I, because $S^p = -I$.

The group $\Delta(p,q,\infty)$ is commensurable to $\mathrm{SL}_2(\mathbb{Z})$ if and only if $K_{pq}=\mathbb{Q}$. The remaining triangle groups are nonarithmetic. For more on triangle groups, see [Tak] and [MR, Ex. 4.9]).

APPENDIX B. ACCIDENTAL ISOMORPHISMS

This supplement describes all overlaps between the series of known primitive Teichmüller curves.

Theorem B.1. The only overlaps between the three series W_D , the two series A_D and G_D , the series V_{pq} and the sporadic series (E_6, E_7, E_8) are the following:

- (1) in genus g = 2, $W_5 = V_{2,5}$ and $W_8 = V_{2,8}$;
- (2) in genus g = 3, $W_8 = V_{3,4}$ and $W_{12} = E_6$; and
- (3) in genus g = 4, $W_5 = V_{3,5}$ and $G_{12} = V_{3,6}$.

Proof. The curves in the five horizontal series indexed by D are all different, since they are generated by forms in different strata. Moreover E_7 and E_8 belong to no other series, since their Veech groups do not contain -I while the others do. Thus we are reduced to identifying overlaps involving E_6 , and coincidences between the vertical series V_{pq} and one of the 5 horizontal series.

In fact, the proof of Theorem 6.4 already shows that E_6 is the same as the Weierstrass curve W_{12} in genus 3; see Figure 6.2. The value D=12 can be checked



FIGURE B.1. A folded triangle that tiles a symmetric pyramid.

using the fact that the order 12 element in the Veech group $\Delta(6, \infty, \infty)$ of E_6 has trace $2\cos(2\pi/12) = \sqrt{3}$, which generates the maximal order in $\mathbb{Q}(\sqrt{3})$.

Next we consider overlaps between W_D and V_{pq} . A coincidence occurs here if and only if the curve V_{pq} has quadratic trace field, its stratum has the form $\Omega \mathcal{M}_g(2g-2)$, and $g(X/\rho)=g-2$. Examining Table D.1, we find the 5 cases listed above; in all cases, the traces of elliptic elements in the Veech group show D is a fundamental discriminant. This argument also shows that $E_6=W_{12}$ does not occur in the series V_{pq} .

Finally, considerations of strata and trace field show there is a unique remaining candidate for an accidental isomorphism: $G_{12} \cong V_{3,6}$. And in fact this isomorphism can easily be seen geometrically: if we cut a symmetric (1, 1, 1, 9) quadrilateral in half, we obtain two copies of the (1, 2, 9) triangle, which generates $V_{3,6}$.

This shows $V_{3,6}$ is at least a *component* of G_{12} . To see they are equal, one can use, for example, the fact that their Euler characteristics are both -1/2 (cf. Table 8.1).

Remark on E_8 . It is also known that the unfolding of the E_8 triangle lies in ΩZ_a for a = (1, 1, 1, 7); see [EMMW, Rmk. 5 in §5].

This fact can be seen geometrically as follows. Consider the cyclic form $\omega = dx/y$ of type (1,1,1,7) on the curve X defined by $y^5 = (x^3-1)^4$. The flat metric $|\omega|$ makes \mathbb{P}^1_x into a symmetric pyramid P, whose base is an equilateral triangle. The cone angles of P are $2\pi/5$ at the vertices of its base, and $14\pi/5$ at its remaining vertex C.

Let $T \subset P$ be the geodesic triangle with vertices (A, B, C), where A is a vertex of the base of P, and B is its barycenter (see Figure B.1). It is readily verified that T is a (3,5,7) triangle, that P is tiled by six copies of T, and that the unfolding of T gives the form (X, ω) .

Appendix C. Tables of Weierstrass curves

Tables C.1, C.2 and C.3, based on [Mu1], [TZ1] and [TZ2], give the topological invariants of W_D in \mathcal{M}_g for real quadratic discriminants $D \leq 60$ and g = 2, 3, 4. More complete tables can be found in these references. The listed topological invariants are the genus g, the number of elliptic points of order n, denoted e_n , the number of cusps c, and the Euler characteristic χ .

A few points should be kept in mind:

- (1) In genus 2 and 3, W_D has two components when $D \equiv 1 \mod 8$. The given invariants are those for *one* of these components.
- (2) In genus 2, besides the listed orbifold points of order 2, we have $e_5(W_5) = e_4(W_8) = 1$.
- (3) Similarly, in genus 3, we have $e_5(W_5) = e_6(W_{12}) = 1$, and in genus 4 we have $e_5(W_5) = e_6(W_{12}) = 1$.
- (4) For any component V of W_D , the trace field is $K = \mathbb{Q}(\sqrt{D})$ and the stratum of a generator is $\Omega \mathcal{M}_q(2g-2)$.

TABLE C.1. The Weierstrass curves W_D in \mathcal{M}_2 .

D	$g(W_D)$	$e_2(W_D)$	$c(W_D)$	$\chi(W_D)$
5	0	1	1	-3/10
8	0	0	2	-3/4
12	0	1	3	-3/2
13	0	1	3	-3/2
17	0	1	3	-3/2
20	0	0	5	-3
21	0	2	4	-3
24	0	1	6	-9/2
28	0	2	7	-6
29	0	3	5	-9/2
32	0	2	7	-6
33	0	1	6	-9/2
37	0	1	9	-15/2
40	0	1	12	-21/2
41	0	2	7	-6
44	1	3	9	-21/2
45	1	2	8	-9
48	1	2	11	-12
52	1	0	15	-15
53	2	3	7	-21/2
56	3	2	10	-15
57	1	1	10	-21/2
60	3	4	12	-18

Table C.2. The Weierstrass curves W_D in \mathcal{M}_3 .

D	$g(W_D)$	$e_2(W_D)$	$e_3(W_D)$	$c(W_D)$	$\chi(W_D)$
8	0	0	1	1	-5/12
12	0	0	0	2	-5/6
17	0	0	1	3	-5/3
20	0	1	0	4	-5/2
24	0	1	0	4	-5/2
28	0	0	2	4	-10/3
32	0	0	0	7	-5
33	0	0	0	7	-5
40	0	1	2	6	-35/6
41	0	0	1	8	-20/3
44	0	1	2	6	-35/6
48	1	0	0	10	-10
52	1	1	0	12	-25/2
56	1	2	2	6	-25/3
57	1	0	1	11	-35/3
60	2	0	0	8	-10

Table C.3. The Weierstrass curves W_D in \mathcal{M}_4 .

D	$g(W_D)$	$e_2(W_D)$	$e_3(W_D)$	$c(W_D)$	$\chi(W_D)$
5	0	0	1	1	-7/15
8	0	1	1	2	-7/6
12	0	1	0	3	-7/3
13	0	0	2	3	-7/3
17	0	0	1	6	-14/3
20	0	2	1	5	-14/3
21	1	0	1	4	-14/3
24	1	2	0	6	-7
28	1	2	2	7	-28/3
29	1	0	3	5	-7
32	1	2	2	7	-28/3
33	2	0	0	12	-14
37	1	0	4	9	-35/3
40	2	2	2	12	-49/3
41	3	0	1	14	-56/3
44	3	4	2	9	-49/3
45	4	0	0	8	-14
48	4	2	1	11	-56/3
52	4	2	2	15	-70/3
53	4	0	5	7	-49/3
56	6	4	2	10	-70/3
57	7	0	1	20	-98/3
60	8	4	0	12	-28

APPENDIX D. TABLE OF BOUW-MÖLLER CURVES

Invariants of the Bouw–Möller curves $V_{pq}\subset \mathcal{M}_g$, for $2\leq g\leq 6$, are given in Table D.1.

This table is organized into groups by genus, with (p,q) increasing within each group. We note that V_{pq} gives the trivial curve in \mathcal{M}_1 for (p,q)=(2,3),(2,4),(2,6),(3,3) and (4,4), and that $V_{6,6}$ is not primitive; the remaining curves are. For each form (X,ω) generating V_{pq} , there is a unique involution ρ satisfying $\rho^*(\omega)=-\omega$; the last column gives the genus of X/ρ .

The topological invariants of V_{pq} can be read off from its Veech group; for example, every curve has genus zero, and one or two cusps. We use the notation for triangle groups given in Appendix A.

Table D.1. The Bouw–Möller curves $V_{pq} \subset \mathcal{M}_g$ with $2 \leq g(V_{pq}) \leq 6$.

(p,q)	Stratum	$\mathrm{SL}(X,\omega)$	Trace field	$g(X/\rho)$
(2,5)	$\Omega \mathcal{M}_2(2)$	$\Delta(2,5,\infty)$	$\mathbb{Q}(\sqrt{5})$	0
(2,8)	$\Omega \mathcal{M}_2(2)$	$\Delta(4,\infty,\infty)$	$\mathbb{Q}(\sqrt{2})$	0
(2, 10)	$\Omega \mathcal{M}_2(1^2)$	$\Delta(5,\infty,\infty)$	$\mathbb{Q}(\sqrt{5})$	0
(2,7)	$\Omega \mathcal{M}_3(4)$	$\Delta(2,7,\infty)$	$\mathbb{Q}(\cos \pi/7)$	0
(2, 12)	$\Omega \mathcal{M}_3(4)$	$\Delta(6,\infty,\infty)$	$\mathbb{Q}(\sqrt{3})$	0
(2, 14)	$\Omega \mathcal{M}_3(2^2)$	$\Delta(7,\infty,\infty)$	$\mathbb{Q}(\cos(\pi/7))$	0
(3,4)	$\Omega \mathcal{M}_3(4)$	$\Delta(3,4,\infty)$	$\mathbb{Q}(\sqrt{2})$	1
(2,9)	$\Omega \mathcal{M}_4(6)$	$\Delta(2,9,\infty)$	$\mathbb{Q}(\cos \pi/9)$	0
(2, 16)	$\Omega \mathcal{M}_4(6)$	$\Delta(8,\infty,\infty)$	$\mathbb{Q}(\cos \pi/8)$	0
(2, 18)	$\Omega \mathcal{M}_4(3^2)$	$\Delta(9,\infty,\infty)$	$\mathbb{Q}(\cos \pi/9)$	0
(3,5)	$\Omega \mathcal{M}_4(6)$	$\Delta(3,5,\infty)$	$\mathbb{Q}(\sqrt{5})$	2
(3,6)	$\Omega \mathcal{M}_4(2^3)$	$\Delta(3,6,\infty)$	$\mathbb{Q}(\sqrt{3})$	1
(4,6)	$\Omega \mathcal{M}_4(6)$	$\widetilde{\Delta}(2,3,\infty,\infty)$	$\mathbb{Q}(\sqrt{6})$	1
(6,6)	$\Omega \mathcal{M}_4(1^6)$	$\Delta(3,\infty,\infty)$	Q	1
(2,11)	$\Omega \mathcal{M}_5(8)$	$\Delta(2,11,\infty)$	$\mathbb{Q}(\cos \pi/11)$	0
(2,20)	$\Omega \mathcal{M}_5(8)$	$\Delta(10,\infty,\infty)$	$\mathbb{Q}(\cos \pi/10)$	0
(2, 22)	$\Omega \mathcal{M}_5(4^2)$	$\Delta(11,\infty,\infty)$	$\mathbb{Q}(\cos \pi/11)$	0
(4, 8)	$\Omega \mathcal{M}_5(4^2)$	$\widetilde{\Delta}(2,4,\infty,\infty)$	$\mathbb{Q}(\sin \pi/8)$	1
(2, 13)	$\Omega \mathcal{M}_6(10)$	$\Delta(2,13,\infty)$	$\mathbb{Q}(\cos \pi/13)$	0
(2, 24)	$\Omega \mathcal{M}_6(10)$	$\Delta(12,\infty,\infty)$	$\mathbb{Q}(\cos \pi/12)$	0
(2, 26)	$\Omega \mathcal{M}_6(5^2)$	$\Delta(13,\infty,\infty)$	$\mathbb{Q}(\cos \pi/13)$	0
(3,7)	$\Omega \mathcal{M}_6(10)$	$\Delta(3,7,\infty)$	$\mathbb{Q}(\cos \pi/7)$	3
(4,5)	$\Omega \mathcal{M}_6(10)$	$\Delta(4,5,\infty)$	$\mathbb{Q}(\sqrt{3+\sqrt{5}})$	2
(5,5)	$\Omega \mathcal{M}_6(2^5)$	$\Delta(2,5,\infty)$	$\mathbb{Q}(\sqrt{5})$	2

Acknowledgements

I would like to thank M. Bainbridge, J. Boulanger, P. Hooper, P. Hubert, E. Lanneau, M. Möller, R. Mukamel and K. Winsor for many useful and informative discussions.

References

- [Ap] P. Apisa, $GL_2\mathbb{R}$ orbit closures in hyperelliptic components of strata, Duke Math. J. **167** (2018), no. 4, 679–742, DOI 10.1215/00127094-2017-0043. MR3769676
- [ACG] E. Arbarello, M. Cornalba, and P. A. Griffiths, Geometry of algebraic curves. Volume II, Grundlehren der mathematischen Wissenschaften [Fundamental Principles of Mathematical Sciences], vol. 268, Springer, Heidelberg, 2011. With a contribution by Joseph Daniel Harris, DOI 10.1007/978-3-540-69392-5. MR2807457
- [AS] P. Arnoux and T. A. Schmidt, Veech surfaces with nonperiodic directions in the trace field, J. Mod. Dyn. 3 (2009), no. 4, 611–629, DOI 10.3934/jmd.2009.3.611. MR2587089
- [AN] D. Aulicino and D.-M. Nguyen, Rank 2 affine manifolds in genus 3, J. Differential Geom. 116 (2020), no. 2, 205–280, DOI 10.4310/jdg/1603936812. MR4168204
- [Ba] M. Bainbridge, Euler characteristics of Teichmüller curves in genus two, Geom. Topol. 11 (2007), 1887–2073, DOI 10.2140/gt.2007.11.1887. MR2350471
- [BaM] M. Bainbridge and M. Möller, The Deligne-Mumford compactification of the real multiplication locus and Teichmüller curves in genus 3, Acta Math. 208 (2012), no. 1, 1–92, DOI 10.1007/s11511-012-0074-6. MR2910796
- [Bo] J. Boulanger, Central points of the double heptagon translation surface are not connexion points, arXiv: 2009.01748, 2020.
- [Bou] N. Bourbaki, Groupes et algèbres de Lie, Ch. IV-VI, Actualites Scientifiques et Industrielles, 1337, Hermann, Paris, 1968; Masson, Paris, 1981.
- [BM1] I. I. Bouw and M. Möller, Differential equations associated with nonarithmetic Fuchsian groups, J. Lond. Math. Soc. (2) 81 (2010), no. 1, 65–90, DOI 10.1112/jlms/jdp059. MR2580454
- [BM2] I. I. Bouw and M. Möller, Teichmüller curves, triangle groups, and Lyapunov exponents, Ann. of Math. (2) 172 (2010), no. 1, 139–185, DOI 10.4007/annals.2010.172.139. MR2680418
- [Ca] K. Calta, Veech surfaces and complete periodicity in genus two, J. Amer. Math. Soc. 17 (2004), no. 4, 871–908, DOI 10.1090/S0894-0347-04-00461-8. MR2083470
- [CK] M. Costantini and A. Kappes, The equation of the Kenyon-Smillie (2, 3, 4)-Teichmüller curve, J. Mod. Dyn. 11 (2017), 17–41, DOI 10.3934/jmd.2017002. MR3588522
- [DL] D. Davis and S. Lelièvre, Periodic paths on the pentagon, double pentagon and golden L, arXiv:1810.11310, 2018.
- [D] L. DeMarco, The conformal geometry of billiards, Bull. Amer. Math. Soc. (N.S.) 48 (2011), no. 1, 33–52, DOI 10.1090/S0273-0979-2010-01322-7. MR2738905
- [Du] E. Duryev, Teichmuller Curves in Genus Two: Square-tiled Surfaces and Modular Curves, ProQuest LLC, Ann Arbor, MI, 2018. Thesis (Ph.D.)—Harvard University. MR4187609
- [EFW] A. Eskin, S. Filip, and A. Wright, The algebraic hull of the Kontsevich-Zorich cocycle, Ann. of Math. (2) 188 (2018), no. 1, 281–313, DOI 10.4007/annals.2018.188.1.5. MR3815463
- [EMMW] A. Eskin, C. T. McMullen, R. E. Mukamel, and A. Wright, Billiards, quadrilaterals and moduli spaces, J. Amer. Math. Soc. 33 (2020), no. 4, 1039–1086, DOI 10.1090/jams/950. MR4155219
- [Ga] F. P. Gardiner, Teichmüller theory and quadratic differentials, Pure and Applied Mathematics (New York), John Wiley & Sons, Inc., New York, 1987. A Wiley-Interscience Publication. MR903027
- [Go] E. Goujard, Sous-variétés totalement géodésiques des espaces de modules de Riemann, Astérisque 430 (2021), 407–424.
- [GJ] E. Gutkin and C. Judge, Affine mappings of translation surfaces: geometry and arithmetic, Duke Math. J. 103 (2000), no. 2, 191–213, DOI 10.1215/S0012-7094-00-10321-3. MR1760625

- [HMTY] E. Hanson, A. Merberg, C. Towse, and E. Yudovina, Generalized continued fractions and orbits under the action of Hecke triangle groups, Acta Arith. 134 (2008), no. 4, 337–348, DOI 10.4064/aa134-4-4. MR2449157
- [Ho1] W. P. Hooper, Another Veech triangle, Proc. Amer. Math. Soc. 141 (2013), no. 3, 857–865, DOI 10.1090/S0002-9939-2012-11379-6. MR3003678
- [Ho2] W. P. Hooper, $Grid\ graphs\ and\ lattice\ surfaces,$ Int. Math. Res. Not. IMRN 12 (2013), 2657–2698, DOI 10.1093/imrn/rns124. MR3071661
- [Hub] J. H. Hubbard, Teichmüller theory and applications to geometry, topology, and dynamics. Vol. 2: Surface homeomorphisms and rational functions, Matrix Editions, Ithaca, NY, 2016. MR3675959
- [HL] P. Hubert and E. Lanneau, Veech groups without parabolic elements, Duke Math. J. 133 (2006), no. 2, 335–346, DOI 10.1215/S0012-7094-06-13326-4. MR2225696
- [HS1] P. Hubert and T. A. Schmidt, Infinitely generated Veech groups, Duke Math. J. 123 (2004), no. 1, 49–69, DOI 10.1215/S0012-7094-04-12312-8. MR2060022
- [HS2] P. Hubert and T. A. Schmidt, An introduction to Veech surfaces, Handbook of dynamical systems. Vol. 1B, Elsevier B. V., Amsterdam, 2006, pp. 501–526, DOI 10.1016/S1874-575X(06)80031-7. MR2186246
- [Hum] J. E. Humphreys, Reflection groups and Coxeter groups, Cambridge Studies in Advanced Mathematics, vol. 29, Cambridge University Press, Cambridge, 1990, DOI 10.1017/CBO9780511623646. MR1066460
- [KS] R. Kenyon and J. Smillie, Billiards on rational-angled triangles, Comment. Math. Helv. 75 (2000), no. 1, 65–108, DOI 10.1007/s000140050113. MR1760496
- [KMS] S. Kerckhoff, H. Masur, and J. Smillie, Ergodicity of billiard flows and quadratic differentials, Ann. of Math. (2) 124 (1986), no. 2, 293–311, DOI 10.2307/1971280. MR855297
- [KM1] A. Kumar and R. E. Mukamel, Real multiplication through explicit correspondences, LMS J. Comput. Math. 19 (2016), no. suppl. A, 29–42, DOI 10.1112/S1461157016000188. MR3540944
- [KM2] A. Kumar and R. E. Mukamel, Algebraic models and arithmetic geometry of Teichmüller curves in genus two, Int. Math. Res. Not. IMRN 22 (2017), 6894–6942, DOI 10.1093/imrn/rnw193. MR3737325
- [LM] E. Lanneau and M. Möller. Non-existence and finiteness results for Teichmüller curves in Prym loci, Exp. Math., to appear.
- [LN1] E. Lanneau and D.-M. Nguyen, Teichmüller curves generated by Weierstrass Prym eigenforms in genus 3 and genus 4, J. Topol. 7 (2014), no. 2, 475–522, DOI 10.1112/jtopol/jtt036. MR3217628
- [LN2] E. Lanneau and D.-M. Nguyen, Weierstrass Prym eigenforms in genus four, J. Inst. Math. Jussieu 19 (2020), no. 6, 2045–2085, DOI 10.1017/s1474748019000057. MR4167002
- [LNZ] A. Larsen, C. Norton, and B. Zykoski, Strongly obtuse rational lattice triangles, Trans. Amer. Math. Soc. 374 (2021), no. 10, 7119–7142, DOI 10.1090/tran/8415. MR4315599
- [Lei] C. J. Leininger, On groups generated by two positive multi-twists: Teichmüller curves and Lehmer's number, Geom. Topol. 8 (2004), 1301–1359, DOI 10.2140/gt.2004.8.1301. MR2119298
- [Loch] P. Lochak, On arithmetic curves in the moduli spaces of curves, J. Inst. Math. Jussieu 4 (2005), no. 3, 443–508, DOI 10.1017/S1474748005000101. MR2197065
- [MR] C. Maclachlan and A. W. Reid, The arithmetic of hyperbolic 3-manifolds, Graduate Texts in Mathematics, vol. 219, Springer-Verlag, New York, 2003, DOI 10.1007/978-1-4757-6720-9. MR1937957
- [Mas1] H. Masur, Closed trajectories for quadratic differentials with an application to billiards, Duke Math. J. 53 (1986), no. 2, 307–314, DOI 10.1215/S0012-7094-86-05319-6. MR850537
- [Mas2] H. Masur, Hausdorff dimension of the set of nonergodic foliations of a quadratic differential, Duke Math. J. 66 (1992), no. 3, 387–442, DOI 10.1215/S0012-7094-92-06613-0. MR1167101
- [Mas3] H. Masur, Ergodic theory of translation surfaces, Handbook of dynamical systems. Vol. 1B, Elsevier B. V., Amsterdam, 2006, pp. 527–547, DOI 10.1016/S1874-575X(06)80032-9. MR2186247

- [MT] H. Masur and S. Tabachnikov, Rational billiards and flat structures, Handbook of dynamical systems, Vol. 1A, North-Holland, Amsterdam, 2002, pp. 1015–1089, DOI 10.1016/S1874-575X(02)80015-7. MR1928530
- [Mc1] C. T. McMullen, Billiards and Teichmüller curves on Hilbert modular surfaces, J. Amer. Math. Soc. 16 (2003), no. 4, 857–885, DOI 10.1090/S0894-0347-03-00432-6. MR1992827
- [Mc2] C. T. McMullen, Teichmüller curves in genus two: discriminant and spin, Math. Ann. 333 (2005), no. 1, 87–130, DOI 10.1007/s00208-005-0666-y. MR2169830
- [Mc3] C. T. McMullen, Prym varieties and Teichmüller curves, Duke Math. J. 133 (2006), no. 3, 569–590, DOI 10.1215/S0012-7094-06-13335-5. MR2228463
- [Mc4] C. T. McMullen, Teichmüller curves in genus two: torsion divisors and ratios of sines, Invent. Math. 165 (2006), no. 3, 651–672, DOI 10.1007/s00222-006-0511-2. MR2242630
- [Mc5] C. T. McMullen, Dynamics of SL₂(ℝ) over moduli space in genus two, Ann. of Math.
 (2) 165 (2007), no. 2, 397–456, DOI 10.4007/annals.2007.165.397. MR2299738
- [Mc6] C. T. McMullen, Braid groups and Hodge theory, Math. Ann. 355 (2013), no. 3, 893–946, DOI 10.1007/s00208-012-0804-2. MR3020148
- [Mc7] C. T. McMullen, Diophantine and ergodic foliations on surfaces, J. Topol. 6 (2013), no. 2, 349–360, DOI 10.1112/jtopol/jts033. MR3065179
- [Mc8] C. T. McMullen, Teichmüller dynamics and unique ergodicity via currents and Hodge theory, J. Reine Angew. Math. 768 (2020), 39–54, DOI 10.1515/crelle-2019-0037. MR4168686
- [Mc9] C. T. McMullen, Modular symbols for Teichmüller curves, J. Reine Angew. Math. 777 (2021), 89–125, DOI 10.1515/crelle-2021-0019. MR4292865
- [Mc10] C. T. McMullen, Billiards, heights, and the arithmetic of non-arithmetic groups, Invent. Math. 228 (2022), no. 3, 1309–1351, DOI 10.1007/s00222-022-01101-4. MR4419633
- [Mc11] C. McMullen, Letter to Leininger, et al., 13 July 2003.
- [MMW] C. T. McMullen, R. E. Mukamel, and A. Wright, Cubic curves and totally geodesic subvarieties of moduli space, Ann. of Math. (2) 185 (2017), no. 3, 957–990, DOI 10.4007/annals.2017.185.3.6. MR3664815
- [Mo1] M. Möller, Periodic points on Veech surfaces and the Mordell-Weil group over a Teichmüller curve, Invent. Math. 165 (2006), no. 3, 633–649, DOI 10.1007/s00222-006-0510-3. MR2242629
- [Mo2] M. Möller, Variations of Hodge structures of a Teichmüller curve, J. Amer. Math. Soc. 19 (2006), no. 2, 327–344, DOI 10.1090/S0894-0347-05-00512-6. MR2188128
- [Mo3] M. Möller, Affine groups of flat surfaces, Handbook of Teichmüller theory. Vol. II, IRMA Lect. Math. Theor. Phys., vol. 13, Eur. Math. Soc., Zürich, 2009, pp. 369–387, DOI 10.4171/055-1/11. MR2497782
- [Mo4] M. Möller, Shimura and Teichmüller curves, J. Mod. Dyn. 5 (2011), no. 1, 1–32, DOI 10.3934/jmd.2011.5.1. MR2787595
- [Mo5] M. Möller, Prym covers, theta functions and Kobayashi curves in Hilbert modular surfaces, Amer. J. Math. 136 (2014), no. 4, 995–1021, DOI 10.1353/ajm.2014.0026. MR3245185
- [MT] M. Möller and D. Torres-Teigell, Euler characteristics of Gothic Teichmüller curves, Geom. Topol. 24 (2020), no. 3, 1149–1210, DOI 10.2140/gt.2020.24.1149. MR4157552
- [MZ] M. Möller and D. Zagier, Modular embeddings of Teichmüller curves, Compos. Math. 152 (2016), no. 11, 2269–2349, DOI 10.1112/S0010437X16007636. MR3577896
- [Mu1] R. E. Mukamel, Orbifold points on Teichmüller curves and Jacobians with complex multiplication, Geom. Topol. 18 (2014), no. 2, 779–829, DOI 10.2140/gt.2014.18.779. MR3180485
- [Mu2] R. E. Mukamel, Polynomials defining Teichmüller curves and their factorizations mod p, Exp. Math. **30** (2021), no. 1, 19–31, DOI 10.1080/10586458.2018.1488156. MR4223280
- [Nag] S. Nag, The complex analytic theory of Teichmüller spaces, Canadian Mathematical Society Series of Monographs and Advanced Texts, John Wiley & Sons, Inc., New York, 1988. A Wiley-Interscience Publication. MR927291
- [Pu1] J.-C. Puchta, On triangular billiards, Comment. Math. Helv. 76 (2001), no. 3, 501–505, DOI 10.1007/PL00013215. MR1854695
- [Pu2] J.-C. Puchta, Addendum to "On triangular billiards", Preprint, 2021.

- [Sal] G. Salmon, Higher Plane Curves, Hodges, Foster and Figgis, Dublin, 1879.
- [Sch1] R. E. Schwartz, Obtuse triangular billiards. II. One hundred degrees worth of periodic trajectories, Experiment. Math. 18 (2009), no. 2, 137–171. MR2549685
- [Sch2] R. Schwartz, Billiards from the square to the stadium, ICM Proceedings, 2022, to appear.
- [Tak] K. Takeuchi, Arithmetic triangle groups, J. Math. Soc. Japan 29 (1977), no. 1, 91–106, DOI 10.2969/jmsj/02910091. MR429744
- [Th] W. P. Thurston, On the geometry and dynamics of diffeomorphisms of surfaces, Bull. Amer. Math. Soc. (N.S.) 19 (1988), no. 2, 417–431, DOI 10.1090/S0273-0979-1988-15685-6. MR956596
- [TZ1] D. Torres-Teigell and J. Zachhuber, Orbifold points on Prym-Teichmüller curves in genus 3, Int. Math. Res. Not. IMRN 4 (2018), 1228–1280, DOI 10.1093/imrn/rnw277. MR3801461
- [TZ2] D. Torres-Teigell and J. Zachhuber, *Orbifold points on Prym-Teichmüller curves in genus 4*, J. Inst. Math. Jussieu **18** (2019), no. 4, 673–706, DOI 10.1017/s1474748017000196. MR3963516
- [V1] W. A. Veech, Teichmüller curves in moduli space, Eisenstein series and an application to triangular billiards, Invent. Math. 97 (1989), no. 3, 553–583, DOI 10.1007/BF01388890. MR1005006
- [V2] W. A. Veech, Geometric realizations of hyperelliptic curves, Algorithms, fractals, and dynamics (Okayama/Kyoto, 1992), Plenum, New York, 1995, pp. 217–226. MR1402493
- [Vi] M. Viana, Dynamics of interval exchange transformations and Teichmüller flows, Preprint, 2008.
- [Vo1] Ya. B. Vorobets, Plane structures and billiards in rational polygons: the Veech alternative (Russian), Uspekhi Mat. Nauk 51 (1996), no. 5(311), 3–42, DOI 10.1070/RM1996v051n05ABEH002993; English transl., Russian Math. Surveys 51 (1996), no. 5, 779–817. MR1436653
- [Vo2] Ya. B. Vorobets, Plane structures and billiards in rational polyhedra (Russian), Uspekhi
 Mat. Nauk 51 (1996), no. 1(307), 145–146, DOI 10.1070/RM1996v051n01ABEH002769;
 English transl., Russian Math. Surveys 51 (1996), no. 1, 177–178. MR1392678
- [Wa] C. C. Ward, Calculation of Fuchsian groups associated to billiards in a rational triangle, Ergodic Theory Dynam. Systems 18 (1998), no. 4, 1019–1042, DOI 10.1017/S0143385798117479. MR1645350
- [Wr1] A. Wright, Schwarz triangle mappings and Teichmüller curves: the Veech-Ward-Bouw-Möller curves, Geom. Funct. Anal. 23 (2013), no. 2, 776–809, DOI 10.1007/s00039-013-0221-z. MR3053761
- [Wr2] A. Wright, Translation surfaces and their orbit closures: an introduction for a broad audience, EMS Surv. Math. Sci. 2 (2015), no. 1, 63–108, DOI 10.4171/EMSS/9. MR3354955
- [Wr3] A. Wright, From rational billiards to dynamics on moduli spaces, Bull. Amer. Math. Soc. (N.S.) 53 (2016), no. 1, 41–56, DOI 10.1090/bull/1513. MR3403080
- [Wr4] A. Wright, Totally geodesic submanifolds of Teichmüller space, J. Differential Geom. 115 (2020), no. 3, 565–575, DOI 10.4310/jdg/1594260019. MR4120819
- [Y] J.-C. Yoccoz, Interval exchange maps and translation surfaces, Homogeneous flows, moduli spaces and arithmetic, Clay Math. Proc., vol. 10, Amer. Math. Soc., Providence, RI, 2010, pp. 1–69. MR2648692
- [Za] J. Zachhuber, The Galois action and a spin invariant for Prym-Teichmüller curves in genus 3 (English, with English and French summaries), Bull. Soc. Math. France 146 (2018), no. 3, 427–439, DOI 10.24033/bsmf.2766. MR3936530
- A. Zorich, Flat surfaces, Frontiers in number theory, physics, and geometry. I, Springer,
 Berlin, 2006, pp. 437–583, DOI 10.1007/978-3-540-31347-2_13. MR2261104

Mathematics Department, Harvard University, 1 Oxford St, Cambridge, Massachussetts 02138-2901